Tectonics

RESEARCH ARTICLE
10.1029/2020TC006145

Key Points:
- A revised Neoproterozoic and Cambrian age of sedimentary rocks in central Idaho is anchored by a 667 Ma tuff and a 601 Ma gabbro
- These rocks record two-stage Rodinian rifting and development of structural domains similar to those in well-defined modern rift margins
- Pre-rifting heterogeneities in lithospheric rigidity (the Belt basin) influenced the final rift geometry

Supporting Information:
- Supporting Information S1
- Table S1

Correspondence to:
D. T. Brennan,
daniel.brennan1@postgrad.curtin.edu.au

Citation:
Brennan, D. T., Pearson, D. M., Link, P. K., & Chamberlain, K. R. (2020). Neoproterozoic Windermere Supergroup near Bayhorse, Idaho: Late-stage Rodinian rifting was deflected west around the Belt basin. *Tectonics*, *39*, e2020TC006145. https://doi.org/10.1029/2020TC006145

Received 20 FEB 2020
Accepted 9 JUN 2020
Accepted article online 14 JUN 2020

Neoproterozoic Windermere Supergroup Near Bayhorse, Idaho: Late-Stage Rodinian Rifting Was Deflected West Around the Belt Basin

Daniel T. Brennan[1,2], David M. Pearson[1], Paul K. Link[1], and Kevin R. Chamberlain[3,4]

[1]Department of Geosciences, Idaho State University, Pocatello, ID, USA, [2]Earth Dynamics Research Group, School of Earth and Planetary Sciences, Curtin University, Perth, Western Australia, Australia, [3]Department of Geology and Geophysics, University of Wyoming, Laramie, WY, USA, [4]Faculty of Geology and Geography, Tomsk State University, Tomsk, Russia

Abstract Conflicting models of Rodinian rifting have been proposed to explain the recognized variation in the Neoproterozoic and early Cambrian tectonostratigraphic architecture of the western Laurentian margin. However, discrimination among rift models is hampered by limited exposure and metamorphism of the rocks. Southeastern Idaho preserves more than 6 km of Neoproterozoic and Cambrian strata. In contrast, along the inferred continuation of the margin in east central Idaho, correlative rocks are missing across the Lemhi arch. Our field mapping and U-Pb dating studies, located approximately 50 km west of the Lemhi arch unconformity, focused on a succession of regionally extensive rocks that were previously assigned an Ordovician age. We show that ~1.5 km of strata here overlies a ~667 Ma reworked felsic tuff and was intruded by a 601 ± 27 Ma gabbro sill; we thus redesignate these rocks as Cryogenian and Ediacaran in age. These rocks are overlain by a ~1 km thick Ediacaran to middle Cambrian quartzite. Middle Ordovician quartzites overlie these middle Cambrian strata, indicating that though Neoproterozoic and lower Cambrian rocks are present west of the Lemhi arch, upper Cambrian and Lower Ordovician rocks are thin or absent. Comparison of this redesignated section to the closest correlative sections suggests an initial stage of symmetric rifting followed by later asymmetric rifting. We suggest that prerifting ~1,370 Ma magmatism within the Belt basin produced lithospheric rigidity that influenced the final stage of rifting and produced heterogeneity in the geometries of structural domains similar to those documented in other well-defined, modern rift margins.

Plain Language Summary Over hundreds of millions of years, Earth's continents come together and rift apart in a process known as the supercontinent cycle. Approximately 750 Ma, a supercontinent called Rodinia began a prolonged rifting process and eventually formed a new margin to ancient North America. This ancient continental margin is inferred to run through Idaho, connecting ca. 600 Myr old rocks in southeastern and north central Idaho. However, rocks of this age were generally thought to be missing in central Idaho and thus led to disagreements on rifting processes. Our geologic mapping and isotopic dating of rocks near Bayhorse, in central Idaho, has revealed that a ~2.5 km thick package of regionally extensive rocks is actually over 150 Myr older than previously thought and was deposited during Rodinia breakup. Comparison of these newly redefined ca. 600 Myr old rocks to those in southeastern and north central Idaho supports that Rodinian rifting occurred in two stages. The first stage appears similar throughout Idaho. However, the final stage shows more erosion and magmatism in central Idaho. We propose that variations in prerifting crustal rigidity are responsible for the differences in rift geometry. This suggests that ancient rifting processes through Idaho were similar to modern rifting processes.

1. Introduction

Investigations of rifted continental margins have reshaped our understanding of how continental lithosphere accommodates the opening of new ocean basins (e.g., Haupert et al., 2016; Manatschal et al., 2015; Péron-Pinvidic et al., 2013, 2015). A major outcome of these studies is that many rifted margins exhibit spatial heterogeneity in extension magnitude in the along- and across-strike directions that is not easily explained in existing pure shear, simple shear, or composite deformation models (c.f., Lister et al., 1986; McKenzie, 1978; Wernicke, 1985). This heterogeneity is often recorded by variations in the geometry,

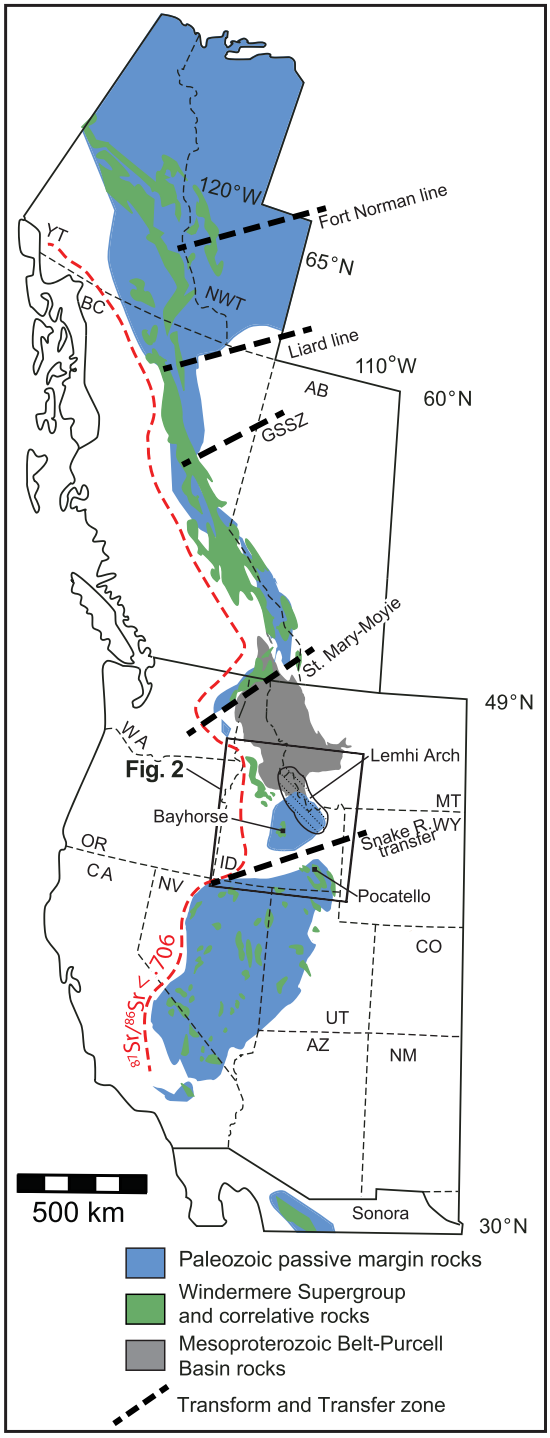

Figure 1. Regional map of the U.S. and Canadian Cordillera showing exposure belts for Mesoproterozoic Belt-Purcell Basin rocks, Neoproterozoic Windermere Supergroup rocks and for Paleozoic passive margin sedimentary rocks, the approximate extent of the Lemhi arch, and transform-transfer zones that were interpreted to separate the miogeoclinal segments of Lund (2008). The $^{87}Sr/^{86}Sr < 0.706$ line approximates the western edge of Laurentia (Armstrong et al., 1977; Elison et al., 1990). Abbreviations: GSSZ = Great Slave Shear Zone; NM = New Mexico; AZ = Arizona; UT = Utah; NV = Nevada; OR = Oregon; WA = Washington; ID = Idaho; MT = Montana; BC = British Columbia; AB = Alberta; YT = Yukon Territory.

facies, and stratigraphic architecture of synrift and postrift strata, which help define structural domains (such as proximal, necking, and distal) that characterize many rifted margins (Péron-Pinvidic et al., 2013).

Neoproterozoic to Cambrian strata of the Windermere Supergroup (J. Stewart, 1972) and its correlatives are exposed intermittently throughout the western North American Cordillera (Figure 1). These rocks record rifting of the supercontinent Rodinia during Cryogenian time which eventually resulted in development of the early Paleozoic western Laurentian passive margin (also referred to as the Cordilleran margin; Bond & Kominz, 1984; Link et al., 1993; Ross, 1991; J. Stewart, 1972; Young et al., 1979). Along much of this margin, consistent detrital zircon progressions and sedimentary facies in Neoproterozoic to lower Paleozoic synrift and passive margin strata have been used to establish regional correlations and understand rifting processes (e.g., Yonkee et al., 2014). However, north of the Snake River Plain in east central Idaho, Neoproterozoic and Cambrian rocks are generally absent. Instead, Ordovician rocks unconformably overlie Mesoproterozoic rocks defining the Lemhi arch (Figure 2, Figure 3; Ruppel, 1986; Scholten, 1957; Sloss, 1954). The documentation by prior workers of major along-strike changes in the western Laurentian rift margin, such as that described in east central Idaho, has stimulated progress in applying end-member models of continental rifting to ancient rift margins. For example, workers have proposed that segmentation and asymmetry of the margin across an ancient northeast striking fault along the modern eastern Snake River Plain (Figure 1) separated rift domains formed above oppositely dipping lithosphere-scale detachment faults ("upper and lower plates;" Link, Todt, et al., 2017; Lund, 2008; Lund et al., 2010). Others (e.g., Beranek, 2017; Campbell et al., 2019) have identified first-order similarities of the western North American rift margin with the hyperextended, magma-poor margins of Newfoundland and Iberia.

Our work, which is focused on rocks exposed southwest of the Lemhi arch in a poorly understood region of central Idaho, significantly refines the geometry and style of Neoproterozoic and Cambrian rifting and initial passive margin sedimentation along the Laurentian rift margin of the northern U.S. Rocky Mountains. Here, Mesozoic and Cenozoic tectonism near Bayhorse, Idaho (Figure 2) has exposed sedimentary and metamorphic rocks near the base of the "passive" margin succession. These rocks were previously considered to be Ordovician in age (e.g., Hobbs et al., 1991). However, new geochronology, provenance analysis, and field-based mapping (Figure 4; Brennan et al., 2020; Krohe et al., 2020) described here indicate an older, Neoproterozoic to Cambrian age. In addition to the new age designation, our work demonstrates a compelling correlation with better-studied rift-related and early passive margin strata exposed elsewhere along the western margin of Laurentia (e.g., Yonkee et al., 2014). Our work fills an important spatial gap in the western Laurentian rift margin, demonstrating that southwest of the Lemhi arch, Neoproterozoic and Cambrian strata record a similar structural domain during continental rifting as other localities to the southeast and northwest. In the context of the western Laurentian margin, our results suggest some similarities with the structural domains documented for other well-defined rift margins such as in the Atlantic and permit new insights into the tectonic evolution of Rodinia and, more broadly, processes of continental rifting. Our work

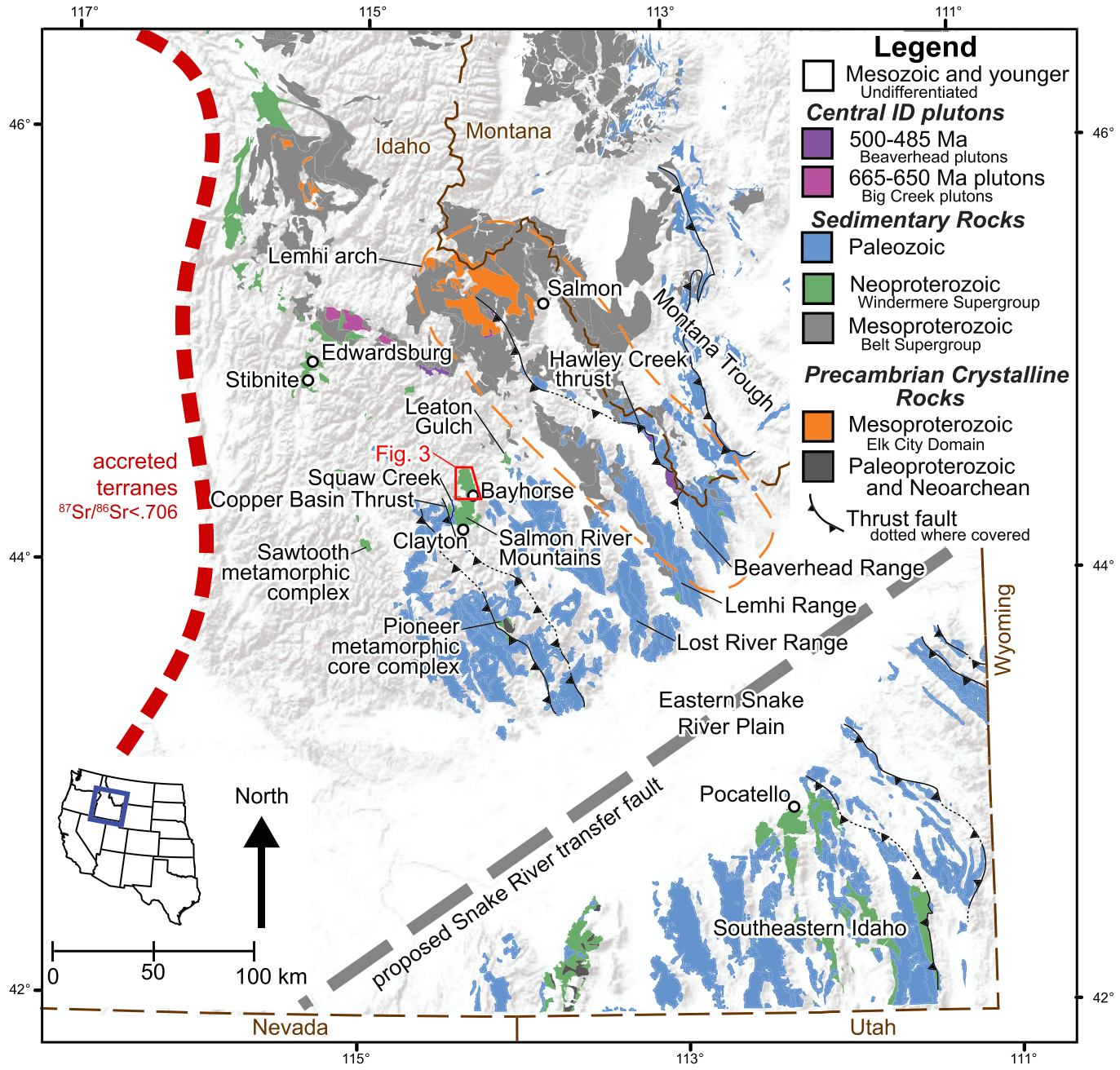

Figure 2. Present-day outcrop map of Paleozoic and older rocks of central and southeastern Idaho. Note the locations of recently documented Neoproterozoic rocks west of the Lemhi arch at Edwardsburg (Lund et al., 2003), Stibnite (D. Stewart et al., 2016), and the Bayhorse region (this study; Brennan et al., 2020; Krohe et al., 2020). The 1:24,000 scale detailed geologic mapping of the Bayhorse region (Brennan et al., 2020) is denoted, of which a simplified map can be seen in Figure 4. Proposed Snake River transfer fault of Lund (2008) and the approximate extent of the Lemhi arch are shown. The $^{87}Sr/^{86}Sr < 0.706$ line approximates the western edge of Laurentia (Armstrong et al., 1977; Elison et al., 1990).

also supports models (e.g., Link, Todt, et al., 2017; Lund, 2008; McMechan, 2012) that implicate the prerifting basement configuration as a major control on along-strike heterogeneities in structural and stratigraphic architecture of the Laurentian rift margin.

2. Geologic Background

Prerift lithospheric ("basement") framework plays a major role in influencing the along-strike heterogeneity of rifted margins (e.g., Buck, 2004; Pereira et al., 2016). In central Idaho, the basement framework consists of

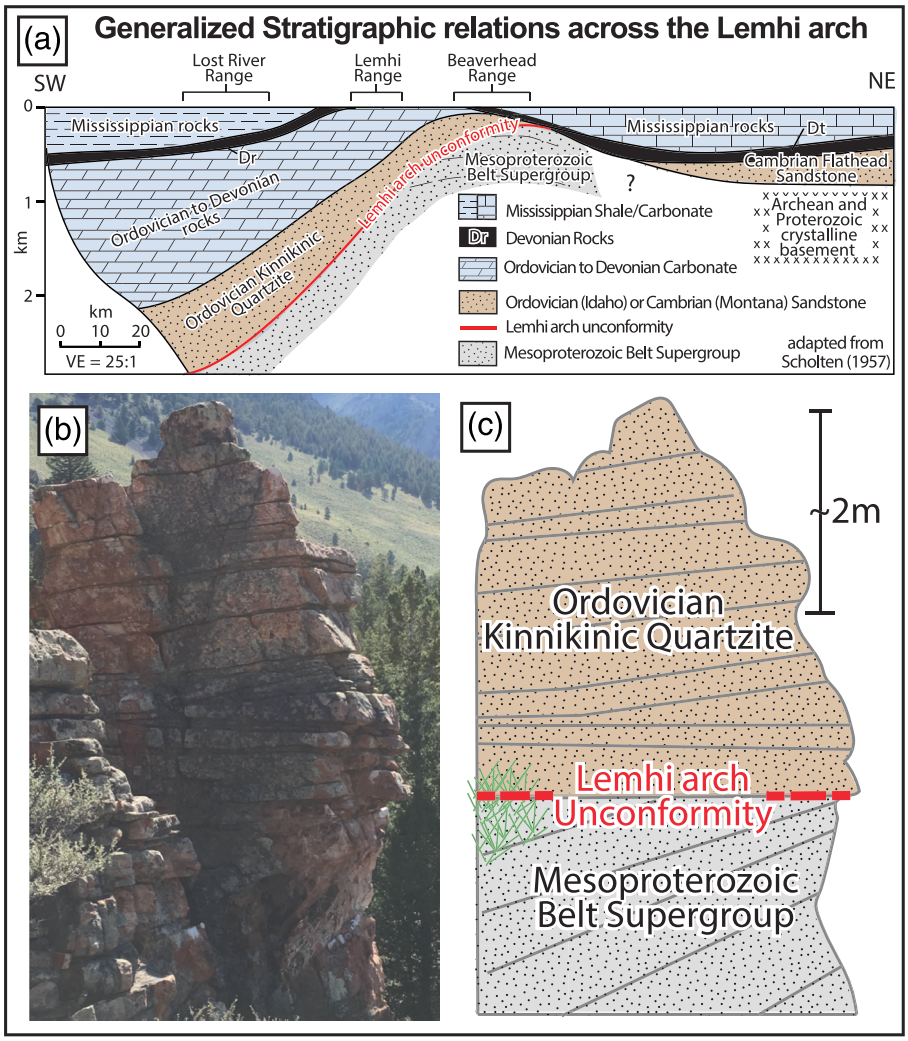

Figure 3. (a) Generalized stratigraphic relations across the Lemhi arch unconformity adapted from Scholten (1957). (b) Field photo of the stratigraphic relationship that defines the Lemhi arch taken in the southern Beaverhead Mountains (Stop 2 of Pearson & Link, 2017). Accompanying sketch (c) showing shallowly dipping Ordovician Kinnikinic Quartzite unconformably overlying steeply dipping Mesoproterozoic Belt Supergroup indicating the absence of Neoproterozoic and Cambrian strata.

two predominantly Neoarchean basement blocks: the Clearwater block in north central Idaho (Vervoort et al., 2016) and the Grouse Creek block in south central Idaho (Link, Autenrieth-Durk et al., 2017). To the east, these Neoarchean blocks abut the Paleo- to Neoarchean Wyoming craton and Medicine Hat block. The Archean origin and association of these four blocks are debated, but they likely share a common history after the Paleoproterozoic assembly of Laurentia (Gaschnig et al., 2013; Mueller et al., 2011). These basement rocks are overlain by Paleoproterozoic quartzites (Neihart Quartzite and its correlatives) and Mesoproterozoic Belt Supergroup strata (Lewis et al., 2010).

Belt Supergroup strata were deposited from ca. 1.47–1.38 Ga in a huge (>200,000 km^2) intracratonic basin that extended across western Montana, east central and northern Idaho, and into eastern Washington and southern British Columbia (Figure 2; Lewis et al., 2010; Link et al., 2016; Price, 1964; Sears, 2007; Winston, 1986). Bimodal plutonism at 1.38 Ga in the southwestern part of the Belt Basin, near Salmon (Figure 2) accompanied late-stage rifting and modification of the lithosphere (Doughty & Chamberlain, 1996). A single ca. 1.38 Ga age peak from inherited zircons within Cretaceous plutons in east central Idaho, near Elk City, suggests that this Mesoproterozoic lithosphere (Elk City domain of Gaschnig et al., 2013) exists under most of the southwestern portion of the Belt basin. On the far western side of Idaho, Laurentia was truncated by

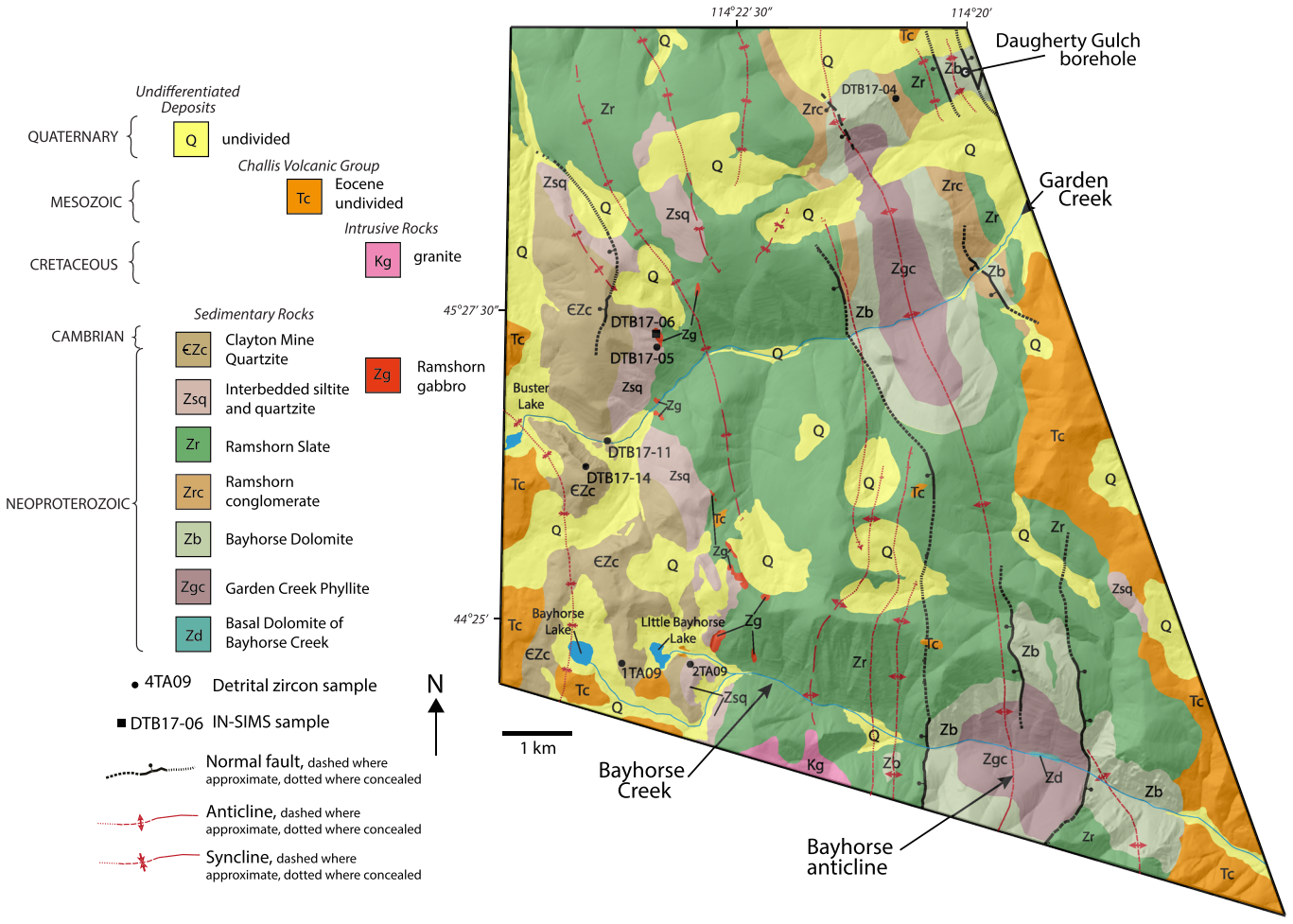

Figure 4. Simplified geologic map (adapted from 1:24,000 scale mapping of Brennan et al., 2020) of the northern portion of the Bayhorse anticline, central Idaho. The Daugherty Gulch borehole containing the Cryogenian 667.8 ± 0.22 Ma (Isakson, 2017) tuff in the northeastern corner of the field area, as well as detrital zircon sample locations, are denoted. Approximately 2.5 km of strata proposed to be Ordovician in age by prior workers (Hobbs et al., 1990) have been reassigned to the Neoproterozoic within this area. IN-SIMS =in situ, secondary ionization mass spectrometry.

Neoproterozoic to early Cambrian rifting during the breakup of Rodinia and now abuts juvenile Paleozoic and Mesozoic provinces accreted in Late Jurassic and Early Cretaceous time (Armstrong et al., 1977; Schwartz et al., 2014).

There is a broad consensus that the western margin of Laurentia formed after a protracted history, involving two main episodes of extension (Beranek, 2017; Bond & Kominz, 1984; Colpron et al., 2002; Levy & Christie-Blick, 1991; Moynihan et al., 2019; Ross & Parrish, 1991; J. Stewart, 1972; Young et al., 1979; Yonkee et al., 2014). The initiation of this prolonged Rodinian rifting was marked by intrusion of the ca. 780 Ma Gunbarrel dikes that occur from northwestern Canada to Wyoming (Harlan et al., 2003). Dike intrusion was followed by formation of localized intracratonic basins and associated siliciclastic sedimentation (Chuar, Uinta Mountain, and Pahrump groups) from ca. 780 to 740 Ma (Dehler et al., 2010, 2017). Deposition of Sturtian diamictite-bearing and generally finer-grained strata (Pocatello Formation and associated units; Figure 5) is generally more widespread and occurred from ca. 720 to 650 Ma during early rifting and volcanism (Link, 1987; Yonkee et al., 2014). Mature siliciclastic rocks of the lower Brigham Group (Caddy Canyon, Inkom and Mutual formations) and its correlatives overlie these older strata and are associated with broad subsidence from 650 to 580 Ma (Link et al., 1987). During this interval, conglomeratic channels within quartzites (above sequence boundary S2; Figure 5; Link et al., 1987) represent Marinoan glacial drawdown (Levy et al., 1994). Final rifting is recorded by unconformably overlying (sequence

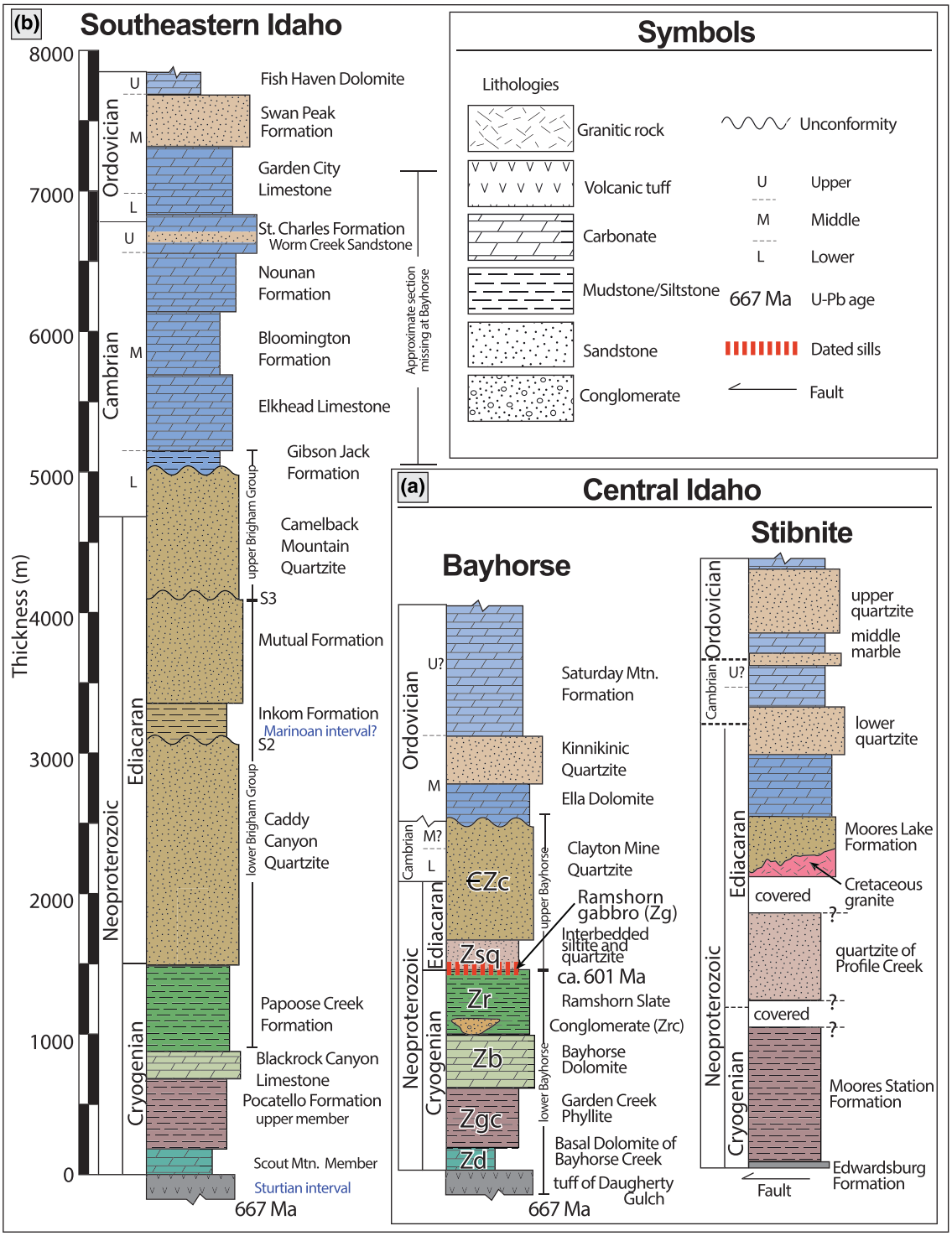

Figure 5. Neoproterozoic to Ordovician stratigraphy of (a) central Idaho at Bayhorse and Stibnite and (b) southeastern Idaho. U-Pb radiometric zircon ages are from Fanning and Link (2004) and Isakson (2017). Southeastern Idaho unit thicknesses are from Trimble (1976) and Link et al. (1987). Stibnite stratigraphy is adapted from Stewart et al. (2016) and Isakson (2017). Bayhorse mapped unit abbreviations (Figure 3) are labeled. Major sequence boundaries (S2 to S3) from Link et al. (1987) are indicated.

boundary S3; Link et al., 1987) siliciclastic, locally arkosic strata of the upper Brigham Group (Camelback Mountain Quartzite and Gibson Jack Formation) and its correlatives, and transition to drift from 570 to 520 Ma (Christie-Blick, 1982; Keeley et al., 2012; Link et al., 1987; Yonkee et al., 2014). Finally, Middle Cambrian to Devonian carbonate-rich strata mark the end of rifting and a transition to regional subsidence along a passive margin (Dickinson, 2004; Link et al., 1993; Mahon et al., 2014; Yonkee et al., 2014).

Lithospheric-scale lineaments (including the northeast trending Snake River transfer zone of Lund, 2008) border most of the significant Cambrian-Ordovician basins of the northern Cordillera, and trend approximately perpendicular to the inferred rift margin (Figures 1 and 2; Cecile et al., 1997; Hayward, 2015; Link, Todt, et al., 2017; McMechan, 2012; Pyle & Barnes, 2003; Roots & Thompson, 1992; Turner et al., 1989). The spatial association of these transfer-transform faults with Proterozoic, Paleozoic, and Cenozoic igneous rocks implies that these structures represent long-lived, leaky zones that were periodically reactivated (Audet et al., 2016; Campbell et al., 2019; Lund, 2008; Millonig et al., 2012).

2.1. The Lemhi Arch

South of the modern Snake River Plain in Idaho and Utah, >6 km of Neoproterozoic and lower Paleozoic strata were deposited on the western margin of Laurentia as part of the Sauk Megasequence (Figure 5; Christie-Blick et al., 1988; Sloss, 1963). However, north of the modern Snake River Plain, in east central Idaho, the Middle Ordovician Kinnikinic Quartzite unconformably overlies tilted Mesoproterozoic Belt Supergroup of the Lemhi subbasin. This unconformity has defined the "Lemhi arch" (Figure 3; Link, Todt, et al., 2017; Ruppel, 1986; Scholten, 1957; Sloss, 1950, 1954), suggesting a significant along-strike change in Laurentian marginal strata across the Snake River Plain (Figure 2).

Less than 50 km northwest of the Lemhi arch, Cryogenian (ca. 665–650 Ma) plutons constitute the Big Creek plutonic suite. Late Cambrian (ca. 500–490 Ma) hypabyssal Beaverhead plutons intruded into Mesoproterozoic Belt Supergroup beneath the Lemhi arch (Lund et al., 2010). Detrital zircons from the Beaverhead plutons are found in nearby upper Cambrian sandstones, which indicate rapid exhumation of the Lemhi arch, and act as a diagnostic signature of uppermost Cambrian (Worm Creek Quartzite and equivalents) strata deposited across southeast Idaho to northwest Wyoming (Link, Todt, et al., 2017). These two discrete magmatic pulses (at 665–650 and 500–490 Ma) indicate recurrent extension along an inherited structural weakness, suggesting a complex rift history (e.g., Lund et al., 2003).

Recent mapping in central Idaho suggests that the Lemhi arch is at least partially a rotated fault block stranded within the margin, which may account for most of the pre-Middle Ordovician tilting of Belt Supergroup within it (Hansen, 2015; Pearson et al., 2016). Cambrian crustal thinning was likely accommodated east of the Lemhi arch, within the central Montana trough (Bush et al., 2012). Prerift Mesoproterozoic (ca. 1.38 Ga) mafic magmatism of the Elk City domain (Doughty & Chamberlain, 1996; Gaschnig et al., 2013) was proposed to have strengthened the lithosphere beneath the arch and played a fundamental control on the lack of preserved Neoproterozoic strata in east central Idaho (Link, Todt, et al., 2017).

2.2. Geology of the Bayhorse Region

Initial work in the Salmon River Mountains (Figure 2; Fisher et al., 1992; Hobbs et al., 1968; Hobbs et al., 1975; Hobbs, 1985; McIntyre et al., 1982; McIntyre & Hobbs, 1987; Patton, 1948; Ross, 1937) established that a section of allegedly lower Paleozoic siliciclastic and carbonate rocks were folded into the N-S trending Bayhorse anticline, intruded by the Cretaceous Idaho batholith and covered by Eocene Challis volcanic rocks. Hobbs and Hays (1990) and Hobbs et al. (1991), who conducted 1:62,500-scale mapping of the region, assigned many of the rocks within the area as Ordovician. However, this age designation was based on a series of miscorrelations made during early exploration of these rocks (i.e., Ross, 1937), and led to mapping of a series of structural-stratigraphic blocks separated by thrust faults (Hobbs et al., 1991). More recent work discovered a reworked tuff at the bottom of a ~1.1 km deep borehole (Jacob, 1990) near the northeastern extent of the Bayhorse anticline (Figure 4). Zircon U-Pb studies of this "tuff of Daugherty Gulch" yielded an age of 664 ± 6 Ma (secondary ionization mass spectrometry; SIMS), interpreted as the time of deposition of the tuff (Lund et al., 2010). However, the stratigraphic and structural context of the tuff were poorly constrained and its implications for the age of rocks near Bayhorse were unknown.

Paleozoic and older rocks within the Bayhorse anticline (including the Clayton Mine Quartzite) crop out over ~300 km^2 and are part of the central Idaho fold-thrust belt. The Bayhorse anticline occurs in the

footwall of the Copper Basin and inferred Squaw Creek thrusts to the west. These thrusts carried Mississippian Copper Basin Group and underlying rocks likely equivalent to those of the Bayhorse anticline. The Bayhorse anticline occurs in the hanging wall of the Hawley Creek thrust (Figure 2; Lewis et al., 2012; Beranek et al., 2016). A ~1.5 km thick section of primarily siliciclastic sedimentary rocks at Leaton Gulch (approximately 25 km to the northeast of Bayhorse; Figure 2) underlie Ordovician units (McIntyre & Hobbs, 1987); the relatively coarse grain size and stratigraphic position of these rocks suggest that they are likely partially correlative to the Clayton Mine Quartzite exposed near Bayhorse (Montoya, 2019). Detrital zircons from the ca. 500–490 Ma Beaverhead plutons are found within the upper Cambrian-Lower Ordovician strata at Leaton Gulch, suggesting that this region was west of the eroding Lemhi arch (Link, Todt, et al., 2017).

Approximately 60 km to the south of Bayhorse, Paleogene extension associated with formation of the Pioneer metamorphic core complex exposed a section of metasedimentary rocks that were interpreted to include the Clayton Mine Quartzite and underlying calc-silicate, gneissose quartzite, and pelitic schist units; these rocks were tentatively assigned a Meso(?)-Neoproterozoic to lower Paleozoic age (Dover, 1981, 1983).

3. Methods

3.1. Field Mapping, Stratigraphic, and Structural Analysis

Standard geologic field mapping practices were used to identify major structural or stratigraphic discontinuities within the field area and to assess potential stratigraphic correlations of rocks within and outside of the study area. Samples for geochronology were collected in the context of 1:24,000-scale field mapping and stratigraphic and structural analyses; a simplified geologic map of the Bayhorse area is given in Figure 4. We also report results collected in the context of recent mapping in the southern part of the adjacent Clayton quadrangle (Krohe et al., 2020). For simplicity, we refer to both map localities as the Bayhorse area. Additional detrital zircon samples outside the Bayhorse-Clayton map areas were collected in the Pioneer Mountains from a metamorphosed section of rocks mapped as Clayton Mine Quartzite and underlying schist (Dover, 1981, 1983). In total, 21 samples were collected (detailed sample localities are given in supporting data Table S1). One igneous (Ramshorn gabbro) sample was analyzed for geochronology (complete results given in supporting data Table S2), and 20 (meta-)sedimentary samples were analyzed for detrital zircon geochronology (complete results given in supporting data Tables S3-S5).

3.2. In Situ-SIMS Analysis of Baddeleyite

Gabbro sills intruded into and were folded with the upper Ramshorn Slate in the Bayhorse section. Attempts to isolate zircon or baddeleyite (ZrO_2) using standard methods were not successful, so X-ray mapping of zirconium in a polished thin section was utilized to determine if zircon or baddeleyite were present. Thin section mapping revealed that baddeleyite grains from 5 to 40 μm in length were present with varying degrees of alteration to zircon (Figure 6). Attempts to separate baddeleyite following the methodology of Söderlund and Johansson (2002) were not successful. Thus, target regions of the polished thin sections were cut out and remounted in a ~2.54 cm diameter epoxy disk along with reference materials. These were analyzed at the University of California-Los Angeles (UCLA) on the CAMECA *ims* 1,290 SIMS, following the methodology of Schmitt et al. (2010) and Chamberlain et al. (2010), using a 1 μm primary O_2^- ion beam, rastered over areas of 3 × 3 μm.

In situ dating of microbaddeleyite crystals (grains too small for separation, generally <50 μm) is complicated by crystal orientation or twinning effects on ionization efficiencies between U and Pb (Wingate & Compston, 2000). U-Pb dates from samples <1.0 Ga often have uncertainties of 2–7% due to crystal orientation bias, but the effects appear to be normally distributed, so mean dates from a large number of analyses of randomly oriented grains are still accurate (Chamberlain et al., 2010; Schmitt et al., 2010). Additional analytical details can be found in supporting information Table S3.

3.3. Detrital Zircon U-Pb Geochronology and Hf Isotope Geochemistry

Zircon crystals were extracted from samples using traditional crushing and grinding methods, followed by separation with a Wilfley table, heavy liquids, and a Frantz magnetic separator. Following separation, zircon grains were incorporated into a 1 inch epoxy mount along with fragments or loose grains of Sri Lanka (SL),

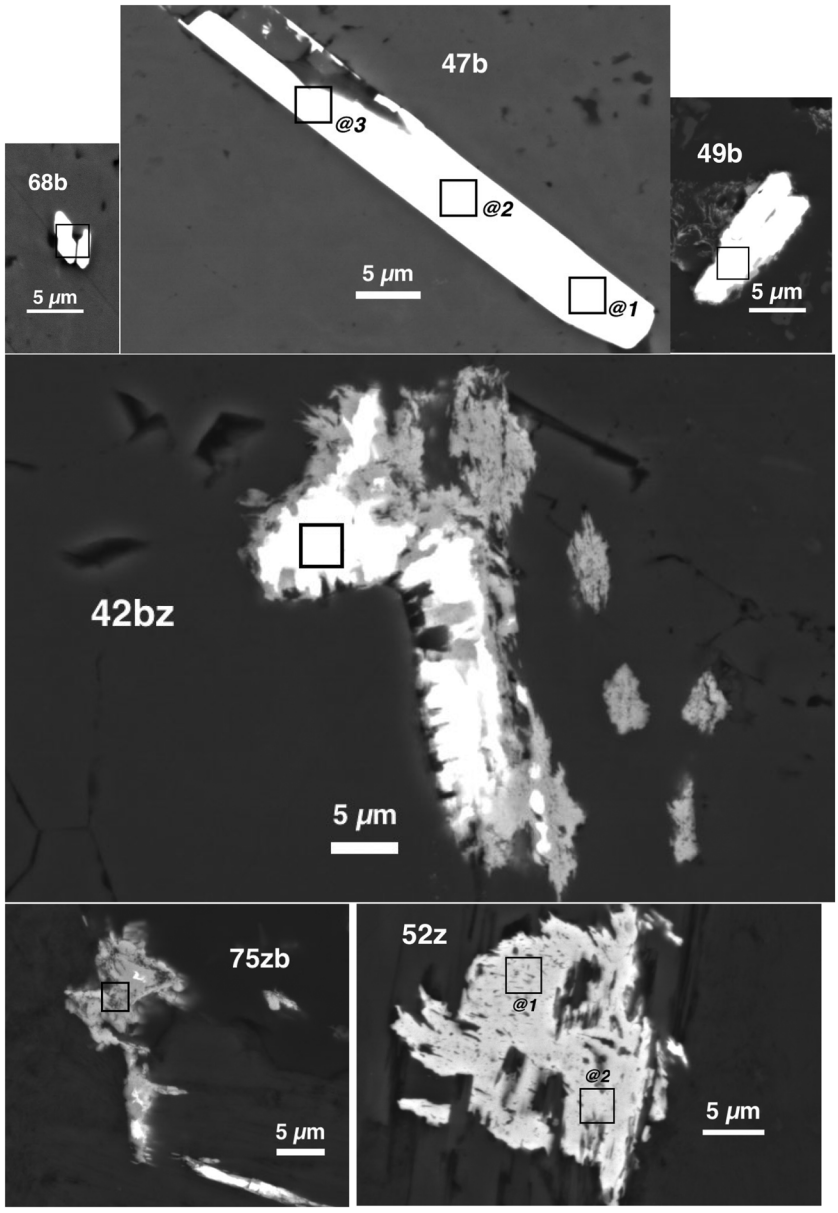

Figure 6. Back-scattered electron (BSE) images of target baddeleyite (b-bright white) and zircon (z-gray) grains and domains dated by in situ SIMS U-Pb methods from Ramshorn gabbro sample DTB17-06. Black squares represent the approximate locations and sizes (3 × 3 μm rasters) of the SIMS analytical spots. Grains 68b and 47b (upper left) represent pure baddeleyite without any apparent zircon alteration; 49b (upper right) has thin zircon rims. The weighted mean $^{206}Pb/^{238}U$ date of the Ramshorn gabbro is based on nine spots from grains like these, all which had Th/U of less than 0.2 (supporting information Table S2). Grains 42bz and 75zb are examples of primary baddeleyite with varying degrees of alteration to zircon; the SIMS analytical spots targeted single-phase domains. The $^{206}Pb/^{238}U$ dates from these spots do not overlap the date from the more pristine baddeleyite grains, however, and may reflect matrix mismatches compared to the pure reference materials used for U-Pb relative sensitivity calibrations. Grain 52z appears to be pure zircon and could represent either magmatic zircon growth or nearly complete alteration of baddeleyite or a mix of both. However, the dates from the two spots vary by nearly 400 Ma and are not interpreted.

FC-1, and R33 zircon crystals. The mounts were sanded down to a depth of ~20 μm, polished, imaged, and cleaned prior to isotopic analysis.

Zircons were analyzed for U-Pb geochronology at the Arizona LaserChron Center using methods outlined by Gehrels et al. (2006, 2008) and Gehrels and Pecha (2014). U-Pb isotope analysis to constrain the age spectra and provenance of the studied stratigraphic sections was conducted using laser ablation inductively

coupled plasma mass spectrometry (LA-ICP-MS) of the unknown zircons. Samples DTB17-04, DTB17-05, DTB17-11, DTB17-17, DTB17-18, DTB17-19, 5NK15, 10NK15, 17NK15, and 4PL14 were analyzed using an Element2 ICP-MS (single collector), which sequences rapidly through U, Th, and Pb isotopes. The analytical sequence consisted of a sample-bracketing procedure with primary and secondary reference materials (SL and FC-1, respectively) analyzed every five unknowns; several R33 secondary reference materials were also analyzed over the course of each sample's analysis. Further analytical details for the Element2 ICPMS analyses are described in Table S3 and Pullen et al. (2018). Samples 1TA09, 2TA09, 3TA09, 4TA09, and 5TA09 were analyzed with a Nu HR ICPMS (multicollector) and U, Th, and Pb isotopes were measured simultaneously. The analytical sequence consisted of a sample-bracketing procedure with a primary reference material (SL) analyzed every five unknowns; R33 was analyzed as a secondary reference material. Further analytical details for the Nu HR ICPMS analyses are described in Table S3 and Gehrels and Pecha (2014).

Data reduction was performed with an Arizona Laserchron python decoding routine and an Excel spreadsheet (E2agecalc). Isoplot, a Microsoft Excel "add-in" program (Ludwig, 2003) and DZstats2.2, a MATLAB-based code (Saylor & Sundell, 2016) were used for generating normalized probability density plots (PDPs). A maximum discordance filter of 20% for normal discordance and 5% for negative discordance was applied. $^{206}Pb/^{238}U$ ages were used for grains younger than 1,000 Ma, $^{207}Pb/^{206}Pb$ ages were used for grains older than 1,000 Ma.

To evaluate the isotopic composition of the source rocks from which the zircons were derived and to further constrain the provenance of key, possibly locally sourced, detrital age-populations, specific detrital grain populations (ca. 665–650 and ca. 1,370 Ma) were also targeted for Hf isotope analysis, using a larger spot diameter of 40 μm located on top of the U-Pb analysis pits. Additional LA-ICP-MS, U-Pb and Hf analytical details can be found in the supporting information Tables S3 and S4.

Three metasedimentary samples from the Clayton Mine Quartzite and the underlying gneissose quartzite and pelitic schist units in the Pioneer metamorphic core complex (Dover, 1981, 1983) were analyzed using the SHRIMP II at Australian National University, following the methods of Williams (1998) and Link et al. (2005).

3.4. Statistical Comparison of U-Pb Detrital Zircon Results

The cross-correlation coefficient of the PDPs was used as a similarity metric among samples. Using the cross-correlation coefficient, each sample was compared to every other sample in the data set. The cross-correlation coefficient is sensitive to the presence or absence of age peaks and to changes in the relative magnitudes or shapes of the peaks. Saylor and Sundell (2016) suggested that the cross correlation of PDPs is the best metric for evaluating sample similarity of large ($n > 300$) and variable n data sets. As our samples vary from $n = 306$ to $n = 79$, this metric is most appropriate.

Multidimensional scaling (MDS) was utilized to visualize the results of the cross-correlation coefficient and to provide an objective grouping of similar detrital zircon samples. The MDS approach plots the samples in Euclidean space (two or more dimensions) while attempting to honor the differences among samples in the cross-correlation matrix. These results are easiest to visualize in two-dimensional Euclidean space; viewed this way, the distance between samples in the MDS plot is roughly equal to the similarity between the samples, and samples containing similar detrital zircon populations will plot in the same region (see Vermeesch, 2013 and Nordsvan et al., 2020 for further description of MDS).

The addition of normally distributed unimodal synthetic populations aids in visualizing differences among samples on an MDS plot (Spencer & Kirkland, 2016). Synthetic normally distributed data sets with a set standard deviation were generated using Excel's (2016) NORMDIST function. Standard deviations were estimated from published data.

4. Results

4.1. Map Relations

Our mapping documents (Figure 4; Brennan et al., 2020) that an approximately 250 m thick gradational stratigraphic contact, that consists of upward coarsening shale and siltstone to interlayered quartzite, shaly quartzite, and finally predominantly quartzite, marks the transition from the Ramshorn Slate to the

overlying Clayton Mine Quartzite (Figure 5a). These field observations indicate that a relatively structurally intact stratigraphic section exists west from Daugherty Gulch (Figure 4). This section consists of the 667 Ma tuff of Daugherty Gulch (Isakson, 2017; Lund et al., 2010), which is overlain by ~1.5 km of dolostone and argillite that coarsen upward into the ~1 km thick Clayton Mine Quartzite. Small (<100 m) gabbroic sill-like bodies (hereby referred to as the Ramshorn gabbro; Brennan et al., 2020) intruded into the Ramshorn Slate within this gradational contact.

Less than 10 km to the northwest of Clayton near Squaw Creek, a >650 m thick Middle Cambrian and older section is surrounded by younger Quaternary and Eocene deposits (Figure 2; Krohe et al., 2020). Cambrian rocks near Squaw Creek crop out over <6 km^2 and consist of a lower interval of predominantly sandstone with lesser carbonate, which is overlain by a Middle Cambrian shale, variably preserved beneath an unconformity. Overlying this unconformity is a dolostone with brachiopods and conodonts of generalized Ordovician age (Hobbs & Hays, 1990).

4.2. Tuff of Daugherty Gulch

In the northeastern part of the Bayhorse map area, near the Daugherty Gulch borehole, our geologic mapping (Figure 4) revealed that although several small-displacement faults are exposed in the area, there are not any major structures between the dated tuff and the Bayhorse section (Brennan et al., 2020). Instead, our revised stratigraphic section correlates well with the rocks described in the borehole (Jacob, 1990): The tuff is overlain by the basal dolomite of Bayhorse Creek, the Garden Creek Phyllite, and the Bayhorse Dolomite (Figure 5a). U-Pb dating of zircons from this tuff yielded an age of 664 ± 6 Ma, interpreted as the time of deposition of the tuff (Lund et al., 2010). Chemical abrasion thermal ionization mass spectrometry (CA-IDTIMS) yielded an equivalent, though more precise, age of 667.8 ± 0.22 Ma (Isakson, 2017).

4.3. In Situ Analysis of Baddeleyite From the Ramshorn Gabbro

In situ SIMS analysis of the Ramshorn gabbro, which intruded the gradational contact between the lower finer grained units and the Clayton Mine Quartzite, consisted of 28 individual analyses (20 predominantly baddeleyite and 8 predominantly zircon; supporting information Table S1). Many of the baddeleyite analyses had high Th/U values, which are interpreted to reflect minor zircon domains within the ion pits (Figure 6). A Th/U of <0.2 filter was applied, which resulted in 12 robust baddeleyite analyses. A final date of 601 ± 27 Ma was calculated based on a weighted mean of $^{206}Pb/^{238}U$ dates from 9 out of 12 robust baddeleyite analyses (Figure 7) and is interpreted as the age of crystallization. The reported precision (±4.5%) is within the 2–7% precision expected by this method (Chamberlain et al., 2010; Schmitt et al., 2010). Zircon ages mostly overlap with the baddeleyite data but show less precision. Alteration to zircon was likely a late magmatic to slightly postmagmatic process.

4.4. U-Pb Detrital Zircon Results

4.4.1. Bayhorse Section

Twelve detrital zircon samples were analyzed from the Bayhorse section (Figure 8). The stratigraphically lowest four samples (DTB17-04, 10NK15, 2TA09, and DTB17-19) were collected from within the Ramshorn Slate and conglomerate and interbedded siltite and quartzite unit. These samples show significant (>20%) ca. 1.3–1.0 Ga detrital zircon populations along with older, relatively broad populations at ca. 1.4, 1.8–1.6, and ca. 2.5 Ga. Sample DTB17-05 was collected adjacent to a Ramshorn gabbro sill. This sample shows similar detrital zircon age-peaks as the stratigraphically lower samples (DTB17-04, 10NK15, 2TA09, and DTB17-19), with the notable addition of a 665–650 Ma population. The lowest sample from the overlying Clayton Mine Quartzite (DTB17-11) shows a dominant (>30%) 665–650 Ma population, with a notable lack of ca. 1.3–1.0 Ga grains but presence of older age peaks at ca. 1,450 and 1,720 Ma. The next stratigraphically higher samples (4PL14 and DTB17-18) show significant (>20%) ca. 1.3–1.0 Ga detrital zircon populations along with older, relatively broad populations at ~1.4, 1.8–1.6, and ca. 2.5 Ga. Up-section within the upper Clayton Mine Quartzite (samples DTB17-14, 1TA09, and DTB17-17) there is a progressive loss of ca. 1.3–1.0 Ga grains, with a switch to a dominant ca. 1,780 Ma age-peak. The uppermost sample (5TA09), from the Middle Ordovician Kinnikinic Quartzite, shows a dominant ca. 1,860 Ma peak.

4.4.2. Squaw Creek Section

Five detrital zircon samples were collected from the Squaw Creek section (Figure 8). Samples 15NK15 and 3TA09, collected from quartzite beds near the base of the section, contain four and three grains each of ca.

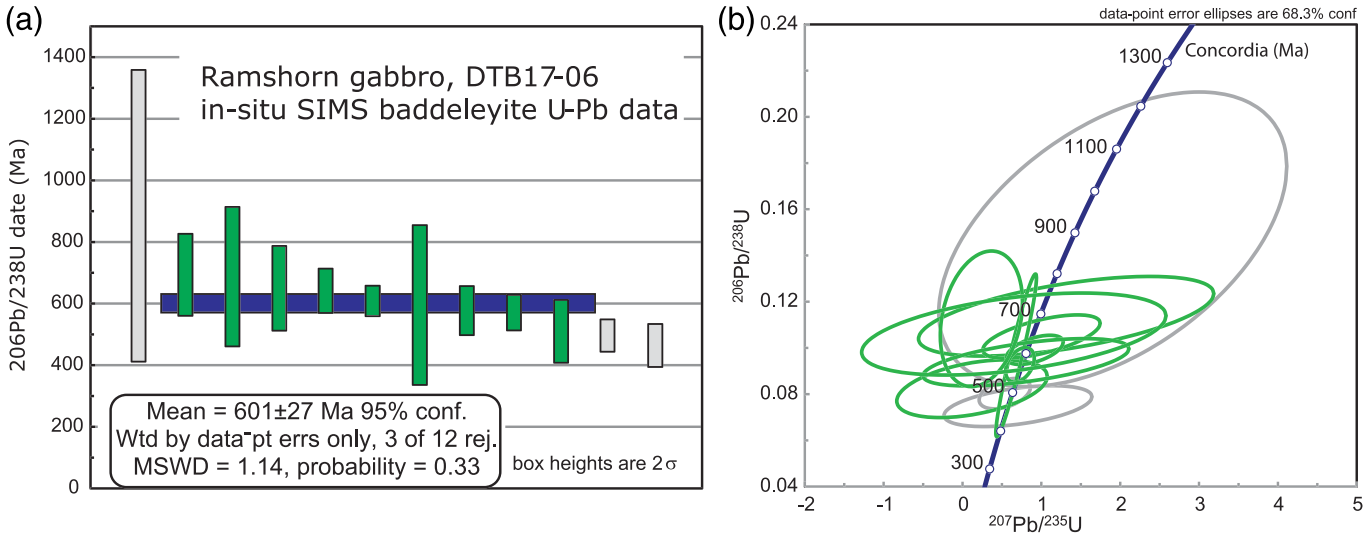

Figure 7. (a) $^{206}Pb/^{238}U$ dates of 12 of the most robust baddeleyite analyses from the Ramshorn gabbro. Weighted mean date is from nine (dark gray) with the other three rejected (light gray) as age outliers. MSWD = mean square weighted deviation (in medium gray). (b) Wetherill concordia plots of analyses shown in Figure 7a. Green circles were included in the age calculation; gray circles were omitted.

670–650 Ma zircon grains along with groups of 1.3–1.0 Ga, ca. 1.4, 1.8–1.6, and ca. 2.5 Ga grains. Stratigraphically higher in the section (within the Cash Creek Quartzite), above a ~400 m thick sandy-carbonate interval and below a Middle Cambrian shale (Hobbs & Hays, 1990), samples 5NK15 and 4TA09 show a complete absence of ca. 1.3–1.0 Ga grains and a switch to a significant ca. 1,780 Ma age-peak. This interval is unconformably overlain by an Ordovician carbonate that contains detrital zircon populations with a dominant ca. 1,860 Ma age peak.

4.4.3. Pioneer Metamorphic Core Complex

Three samples (1PL08, 5PL08, and 6PL08) of metasedimentary rocks (a pelitic schist, conglomeratic quartzite, and a calc-silicate) from the middle plate of the Pioneer metamorphic core complex (Dover, 1983; Link, Autenrieth-Durk, et al., 2017; supporting information Table S5) yielded 70 grains less than 15% discordant. The lumped results from these samples show sparse Archean grains, a Paleoproterozoic mode at ca. 1,780 Ma, sparse Mesoproterozoic grains (ca. 1.4 Ga) and a broad population at ca. 1.3–1.0 Ga (Figure 9).

4.5. Detrital Zircon Provenance Groups

Based on geological information, visual comparison of the probability density plots (Figures 8 and 9) and the results of the MDS cross-correlation pattern (Figure 10) we consider the detrital zircon samples to indicate four separate provenance "groups" as discussed below. Due to the different analytical method used for the Pioneer metamorphic core complex samples (SIMS) compared to the remainder of the data set (LA-ICP-MS), they were not included in the MDS statistical comparison (e.g., Nordsvan et al., 2020) and were grouped entirely on geological information and visual comparison of probability density plots.

4.5.1. Group A

Group A consists of samples from the lower Bayhorse sequence (DTB17-04, 10NK15, 2TA09, DTB17-19, 4PL14, and DTB17-18), the lower sample from the Squaw Creek section (Quartzite of Boundary Creek; 15NK15) and from the Pioneer metamorphic core complex (1PL08, 6PL08, and 5PL08). These samples all show significant ca. 1.3–1.0 Ga detrital zircon populations along with older, relatively broad populations at ~1.4, 1.6–1.8, and ca. 2.5 Ga. The abundance of 1.3–1.0 Ga grains defines this group.

4.5.2. Group B

Within the Bayhorse section, Group B contains samples from the upper Clayton Mine Quartzite (1TA09, DTB17-17, and DTB17-14). Group B also contains samples from the Squaw Creek section within the Cash Creek Quartzite (3TA09, 5NK15, and 4TA09). The relative absence of ca. 1.3–1.0 Ga grains and a significant unimodal ca. 1780 age peak define this group. One of the stratigraphically highest samples (DTB17-14) yielded a single Cambrian age at 529 ± 6 Ma.

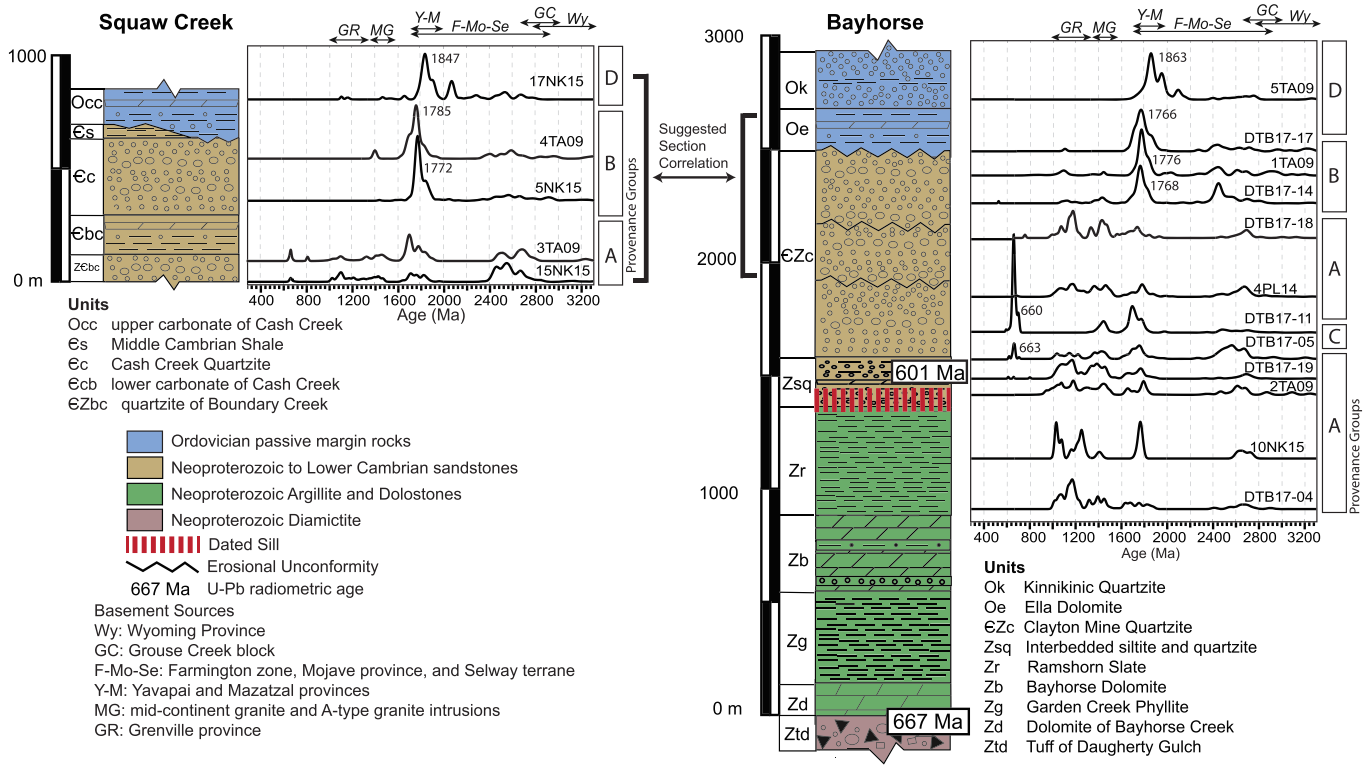

Figure 8. Lithostratigraphic columns of the Bayhorse and Squaw Creek sections with normalized probability density plots at their respective stratigraphic position on the right. Significant unimodal age peaks are labeled. Both stratigraphic sections are interpreted to record the rise of the Transcontinental Arch in early Cambrian time and disappearance of Grenville grains; this suggests that the more complete Squaw Creek section was thrust upon the (albeit slightly more complete) Clayton Mine Quartzite correlative. Provenance groups (see Figure 10) are indicated on the right of the probability density plots. Sample locations and data can be found in supporting information Tables S1 and S3.

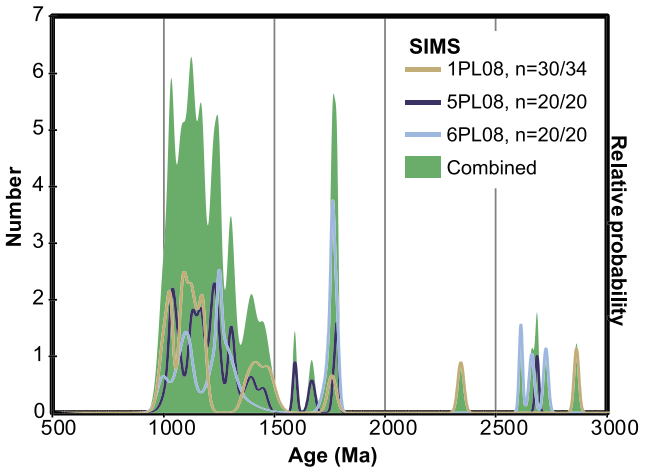

Figure 9. Probability density plot of samples 1PL08 (tan), 5PL08 (purple), 6PL08 (light blue), and combined (green) from the middle plate of the Pioneer metamorphic core complex showing 70 concordant analyses. These samples were analyzed on the SHRIMP at Australian National University. We interpret these samples to show a similar provenance to Bayhorse provenance Group A (see Figure 10).

4.5.3. Group C

Group C, with one sample (DTB17-11 from the lower Clayton Mine Quartzite), is characterized by abundant ca. 670–650 Ma zircon grains, groups of ca. 1.4 and 1.8–1.7 Ga grains, and lack of 1.3–1.0 Ga grains. DTB17-11 also has a few grains with ages <650 Ma, which could reflect Pb loss or may bracket the maximum depositional age.

Other samples from the lower Clayton Mine Quartzite (DTB17-05) and from correlative strata in the Squaw Creek section (15NK15 and 3TA09) also contain limited numbers of 670–650 Ma grains. Objectively, due to similar stratigraphic positions and the presence of Neoproterozoic grains these samples could also be considered part of this Group C, as K-S test D value analysis suggests (see supporting information Table S7). However, DTB17-05 and 15NK15 also contain ca. 1.3–1.0 Ga grains and thus are discussed as part of Group A. 3TA09 does not contain ca. 1.3–1.0 Ga grains and thus is discussed as part of Group B. Alternatively, these samples could also be considered as showing a mixed provenance between groups A, B, and C.

4.5.4. Group D

Group D contains the Middle Ordovician Kinnikinic Quartzite and correlatives, which has the same detrital zircon age assemblage from central Idaho to central Nevada (Beranek et al., 2016). Both samples 5TA09 (Kinnikinic Quartzite from the Bayhorse anticline) and 17NK15 (Ordovician carbonate of the Squaw Creek section) show the youngest age-peak to be ca. 1,860 Ma.

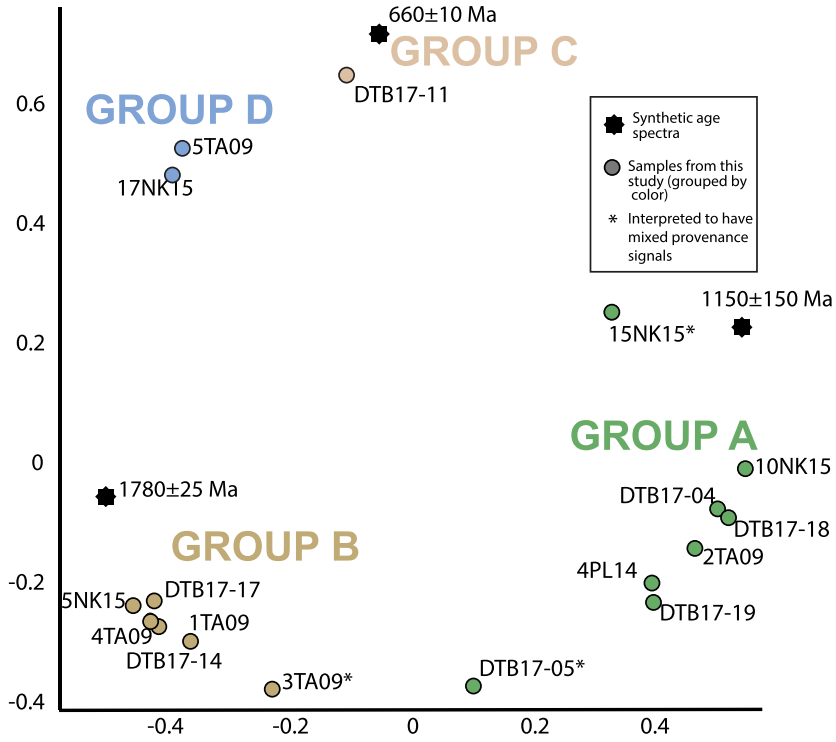

Figure 10. Nonmetric, multidimensional scaling plot of detrital zircon age spectra (see Vermeesch, 2013) of samples from this study (circles) and synthetic age populations (stars, $n = 100$ with the 2 sigma standard deviations indicated). Plot is based on the cross-correlation metric; the axes are arbitrarily calculated values to illustrate similarity of each data set in 2-D space (Saylor & Sundell, 2016). Thus, points that plot closer together are statistically more similar. We interpret the detrital zircon results from the Bayhorse region to show four distinct provenance groupings (Groups A–D). Samples DTB17-05, 3TA09, and 15NK15 are interpreted to show a mixed provenance signal.

4.6. Lu-Hf Results

The ca. 660 and 1,370 Ma U-Pb zircon age populations are unique in the northern U.S. Rocky Mountains. Hf isotope geochemistry was thus applied to test the provenance of the ca. 660 and 1,370 Ma grains and to evaluate the isotopic composition of the source rocks from which the zircons were derived. The ca. 660 Ma detrital zircons ($n = 33$) yielded initial εHf values ranging from +7 to 0, indicating an intermediate to moderately juvenile composition (Bahlburg et al., 2011). Ca. 1.38 Ga detrital zircons ($n = 21$) yielded initial εHf values ranging from +11 to +1, indicating a moderately juvenile to juvenile composition (Figure 11).

5. Discussion

Neoproterozoic to Cambrian Windermere Supergroup rocks along the western Laurentian margin are generally interpreted to record a two-stage history of continental rifting of Rodinia (Bond et al., 1985; Colpron et al., 2002; Levy & Christie-Blick, 1991; Ross, 1991; Yonkee et al., 2014). Various models of lithospheric extension (pure shear, simple shear, or depth-dependent extension models) have been applied to the western Laurentian margin to explain some of the spatial and temporal heterogeneities in these rocks (e.g., Beranek, 2017; Bond et al., 1985; Lund, 2008; Yonkee et al., 2014). In their study focused on rift-related Neoproterozoic and Cambrian rocks exposed in northern Utah and southeastern Idaho, Yonkee et al. (2014) advocated for a shift from pure-shear extension during early rifting followed by a second stage of depth-dependent extension. Recent work on similar rocks along the western Laurentian margin (e.g., Beranek, 2017; Campbell et al., 2019; Moynihan et al., 2019) has also suggested a broad analog of Rodinian rifting to better-constrained models of rifting described for opening of the Atlantic Ocean. However, an incomplete and fragmented geologic record of these events along the projected continuation

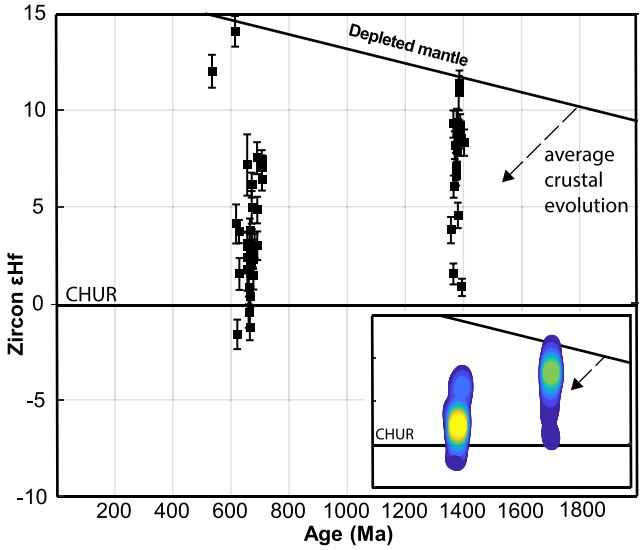

Figure 11. Detrital zircon (n = 54) initial εHf values versus age (Ma) (from samples DTB17-14, DTB17-11, DTB17-05, and DTB17-04) results for detrital age populations centered around ca. 650 and 1,370 Ma, with εHf uncertainties shown. Plot in bottom right shows the same data displayed as bivariate kernel density estimates after Spencer et al. (2019). Warmer colors indicate a greater concentration of εHf values. εHf is $^{176}Hf/^{177}Hf$ normalized to CHUR (Bouvier et al., 2008). Depleted mantle curve is based on Vervoort et al. (1999).

of the rift margin between southern Idaho and southern Canada has hindered application of models of rifting to a substantial portion of the margin.

Our mapping and U-Pb dating, in a region of the Cordilleran margin where Neoproterozoic and lower Paleozoic rocks were thought to be absent, indicate that ~1.5 km of strata overlie a ~667 Ma felsic tuff and were intruded by a 601 ± 27 Ma gabbro sill; these rocks are thus Cryogenian and Ediacaran in age. These rocks are overlain by a ~1 km thick Ediacaran to Middle Cambrian quartzite. These results revise the stratigraphic architecture in this area of the Cordilleran margin, and allow proposal of a regional tectonic model for Neoproterozoic to early Paleozoic rifting.

The studied Bayhorse strata are located approximately 150 km inboard from the nearest documented significant strike-slip faults in the western Idaho shear zone (Schmidt et al., 2017) and show a Laurentian provenance. Additionally, the identification of metamorphosed but compositionally similar strata ~100 km to the north at Stibnite and Big Creek (Lund et al., 2010; D. Stewart et al., 2016), ~60 km to the southwest within the Sawtooth metamorphic complex (Ma et al., 2016) and 60 km to the south in the Pioneer Mountains (Figure 2) suggest that the Bayhorse strata are native to central Idaho. Thus, our proposed correlations and tectonic model assumes that the rocks of the Bayhorse region are not an "allochthonous" slice of the Cordilleran margin translated by Mesozoic dextral strike-slip faults, nor part of the proposed accreted ribbon continent "Rubia" (Hildebrand, 2009).

5.1. Early Paleozoic Fossil Constraints

Less than 10 km to the west/southwest of the Bayhorse anticline, the >650 m stratigraphic section preserved near Squaw Creek shows the same stratigraphic provenance trend seen in the upper Bayhorse section (from Group A to Group B) and is conformably overlain by a shale containing trilobites of early to middle Cambrian age (Hobbs et al., 1968; Hobbs & Hays, 1990). This suggests that the Squaw Creek section below the middle Cambrian shale is slightly more complete, and correlative to the upper Clayton Mine Quartzite. Both are likely middle Cambrian and older (Figure 8).

The middle Cambrian shale at Squaw Creek is variably preserved beneath a dolostone with brachiopods and conodonts of generalized Ordovician age (Hobbs & Hays, 1990). Based on stratigraphic position, detrital zircon populations (both Group D) and fossil age similarity, the Ordovician dolostone at Squaw Creek is likely correlative to the Ella Dolomite, which overlies the Clayton Mine Quartzite. This indicates that upper Cambrian and possibly Lower Ordovician strata are likely missing in both the Squaw Creek and Bayhorse sections (Figure 8).

5.2. Provenance of Rocks in the Bayhorse and Squaw Creek Sections

Several studies (e.g., Balgord et al., 2013; Gehrels & Pecha, 2014; Linde et al., 2014; Link, Todt, et al., 2017; Matthews et al., 2018; Yonkee et al., 2014) characterized the provenance of regionally consistent detrital zircon populations found in Neoproterozoic and lower Paleozoic strata along the Cordilleran margin. Apart from the unique 665–650 Ma detrital zircons, the detrital zircon populations from the Bayhorse and Squaw Creek section (Figure 8) fit this well-established framework, and thus only a brief discussion of provenance is presented.

5.2.1. Group A

Group A is characterized by abundant 1.3–1.0 Ga zircon grains likely sourced from the Llano Uplift, Appalachian basement inliers, and Grenville orogen of eastern to southeastern Laurentia (Eriksson et al., 2003; Mueller et al., 2007; Spencer et al., 2014; Whitmeyer & Karlstrom, 2007) and transported west by a Neoproterozoic pancontinental river system (Rainbird et al., 2012). The relatively broad, older Proterozoic age-peaks (ca. 1.35–1.5 and 1.6–1.8 Ga) are consistent with primary derivation from

Laurentian basement present to the east/southeast (midcontinent granite, Yavapai-Mazatzal provinces), or could be recycled through the Belt Supergroup. Several episodes of recycling and minor contributions from the ca. 1.37 Ga Elk City domain are possible. There are several possible sources for the limited Archean grains in Group A, including the Grouse Creek, Clearwater, Wyoming, and Medicine Hat blocks (Foster et al., 2006; Vervoort et al., 2016).

5.2.2. Group B

Provenance Group B shows a prominent ca. 1780 detrital zircon population with lesser Neoarchean populations. Potential sources for the ca. 1,780 Ma grains include (1) the Yavapai province (including the Green Mountain arc of southwestern Wyoming; Jones et al., 2011; Reed et al., 1987) that was exhumed as part of the Transcontinental Arch (Malone et al., 2017), (2) the Swift Current anorogenic province of southwestern Saskatchewan and southeastern Alberta, Canada (Collerson et al., 1988; Linde et al., 2017; Matthews et al., 2018; Ross et al., 1991), and (3) a magmatic suite within the Great Falls tectonic zone (Mueller et al., 2002).

A similar provenance shift (from dominant ca. 1.3–1.0 Ga grains to their relative absence) in age-correlative rocks has been interpreted to signal early Cambrian exhumation of the Transcontinental Arch, a northeast to southwest trending topographic high across the Laurentian midcontinent, and disruption of the pancontinental river system sourcing eastern Laurentia Grenville provinces (Amato & Mack, 2012; Linde et al., 2014; Link, Todt, et al., 2017; Matthews et al., 2018; Rainbird et al., 2017). The single young zircon at 529 ± 6 Ma (1σ; measurement errors only) is consistent with an early Cambrian depositional age but needs to be substantiated with additional analyses.

5.2.3. Group C

Provenance Group C shows a major ca. 660 Ma grain population, a noticeable lack of ca. 1.3–1.0 Ga grains, and older age peaks at ca. 1,450 and 1,720 Ma. These populations are consistent with sourcing from the nearby 665–650 Ma Big Creek plutons and reworking of the surrounding Mesoproterozoic Belt Supergroup. The occurrence of this Cryogenian detrital zircon population is limited to the section adjacent to and just above the ca. 601 Ma Ramshorn gabbro. This may indicate that the ca. 601 Ma period of magmatism was coeval with local exhumation of the rift margin.

It is important to note that another period of magmatism and coeval margin exhumation is observed in central Idaho with Late Cambrian intrusion and subsequent exhumation of the Beaverhead plutons. This event is associated with the distinctive 500–490 Ma detrital zircon populations found in upper Cambrian sandstones deposited across southeast Idaho, Montana and Wyoming (Link, Todt, et al., 2017). No 500–490 Ma detrital zircons were found in the Bayhorse or Squaw Creek sections. However, grains of this age are found near the top of the section at Leaton Gulch and to the north near Stibnite (Figure 2; Isakson, 2017).

5.2.4. Group D

Middle Ordovician units of provenance Group D show detrital zircon populations at ca. 1,860 Ma and a scattering of older Neoarchean ages. This is consistent with provenance from the Peace River Arch and surrounding Trans-Hudson basement of the northern Canadian Shield (Gehrels & Pecha, 2014; Linde et al., 2017).

5.3. Regional Correlations

Metamorphosed Neoproterozoic and Cambrian rocks west of the Lemhi arch in the Sawtooth metamorphic complex, near Stibnite, and at Edwardsburg (Figure 2) likely correlate to the Neoproterozoic and Cambrian rocks at Bayhorse. We suggest that the Moores Station Formation (Figure 12; Lund et al., 2003; D. Stewart et al., 2016) correlates with the lower argillaceous and carbonate interval of the Bayhorse section. The Moores Station Formation is overlain by <1,000 m of quartzite with lesser calc-silicate intervals. Detrital zircon samples from the lower portion of this interval contain significant ca. 1.3–1.0 Ga grains along with a small population of ca. 660 Ma grains (D. Stewart et al., 2016), higher up in the section the ca. 1.3–1.0 Ga grains disappear, and a ca. 1.78 Ga peak is prominent (Isakson, 2017). This interval is interpreted to span the Cambrian/Neoproterozoic boundary and likely correlates to the Clayton Mine Quartzite.

Neoproterozoic to Cambrian sedimentary rocks in northern and southeastern Idaho correlate with the newly reassigned Neoproterozoic to Cambrian strata of the Bayhorse section. In southeastern Idaho, a reworked fallout tuff of the Scout Mountain Member of the Pocatello Formation, with zircons yielding a U-Pb SIMS age of 667 ± 5 Ma (Fanning & Link, 2004), is overlain by ~1.5 km of limestone and argillite

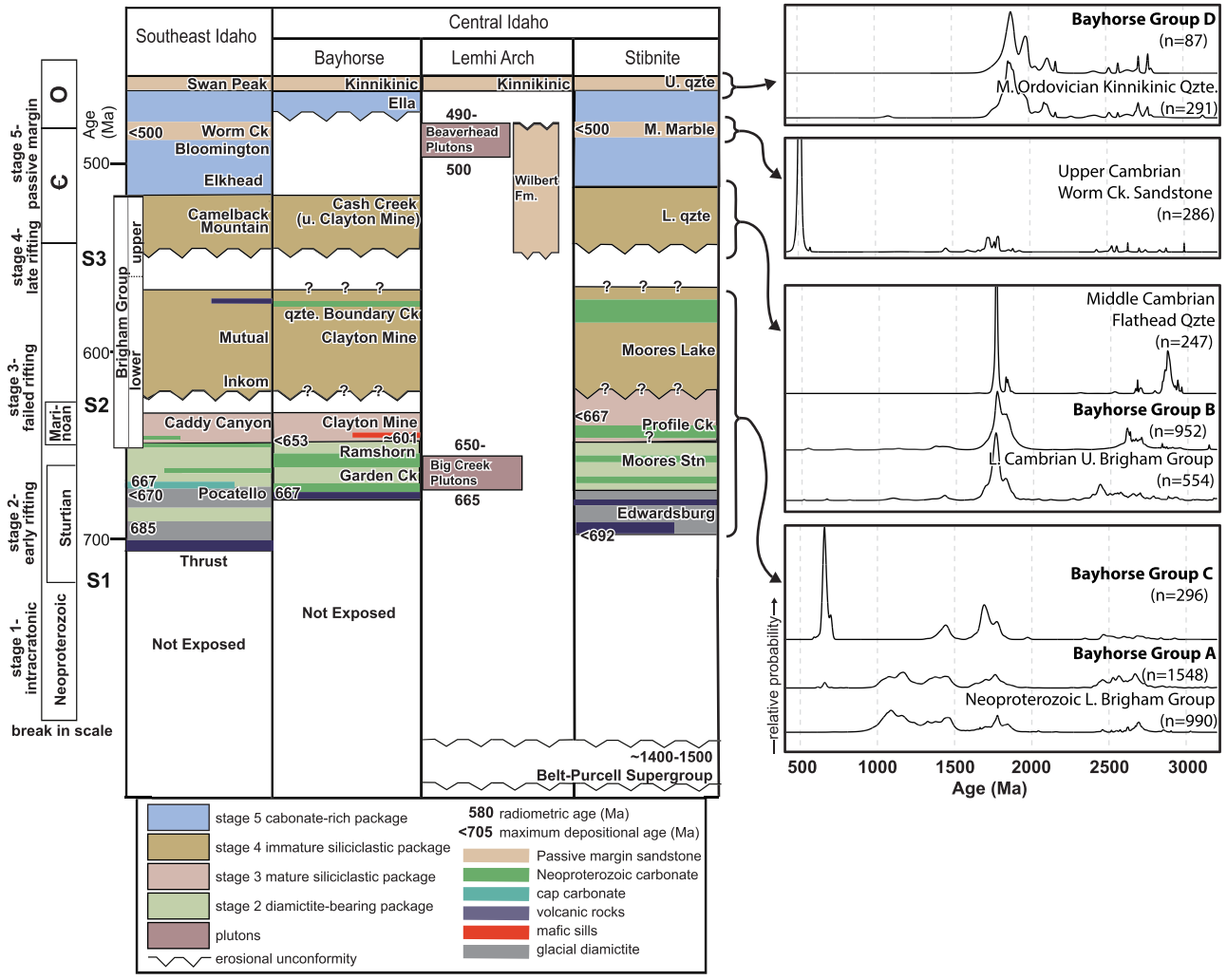

Figure 12. Reference chronostratigraphic sections and published age constraints for Neoproterozoic to Ordovician strata in southeast Idaho (adapted from Balgord et al., 2013 and Yonkee et al., 2014) and proposed correlations of the central Idaho stratigraphy. Stibnite section after Isakson (2017). Along the vertical axis, five stages of rifting from Yonkee et al. (2014) are indicated. Major sequence stratigraphic boundaries (S1 to S3) are indicated (Link et al., 1987); in the southeastern Idaho section, these boundaries occur in the upper Caddy Canyon Quartzite (S2) and above the Mutual Formation (S3). To the right are normalized probability detrital zircon plots for the Bayhorse samples and compiled published data sets of Neoproterozoic to Ordovician strata from southeastern Idaho and correlative strata in northern Utah and northwest Wyoming. Detrital zircon results from the Stibnite section are not shown here but presented in Isakson (2017). Bayhorse samples were grouped based on geologic information and visual comparison of PDPs and MDS groupings (see Figure 10). See supporting information Table S9 for complete list and source of compiled samples.

(Yonkee et al., 2014). In Utah, correlative strata also show a 667 ± 5 maximum depositional age, which likely closely approximates the depositional age (Balgord et al., 2013). Based on matching tuff/volcaniclastic ages and lithological similarity, we correlate this southeastern Idaho interval to the lower Bayhorse section (Figures 5 and 12). Detrital zircon samples above these tuffs in both southeastern Idaho and at Bayhorse (Group A) contain abundant 1.3–1.0 and 1.5–1.35 Ga detrital grains.

In southeastern Idaho, ~3.5 km of Brigham Group quartzites overlie lower carbonate rocks and argillite, while at Bayhorse, the ~1 km thick Clayton Mine Quartzite overlies this interval. The shift in detrital zircon populations within the Clayton Mine Quartzite (from Group A to Group B) and the recognition of a similar provenance shift within several other basal Cambrian sandstones in southeastern Idaho, central Idaho, and southwestern Montana (Matthews et al., 2018), suggest the correlation of the Clayton Mine Quartzite with the Brigham Group quartzites of southeastern Idaho. The lower ~600 m of the Clayton Mine Quartzite has similar detrital zircon populations (Group A) to the lower Brigham Group (Caddy Canyon, Inkom,

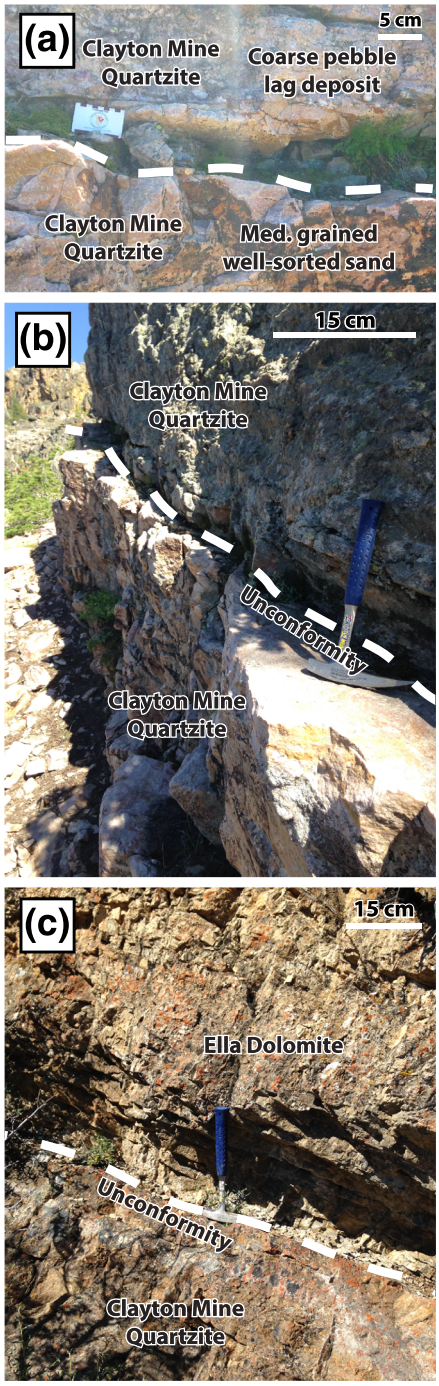

Figure 13. (a and b) Disconformity or low-angle unconformity within the Clayton Mine Quartzite. Dashed lines trace out the probable erosional surface with a coarse pebble deposit overlying a medium-grained, well-sorted sandstone. Along Garden Creek, this unconformity separates the underlying provenance Groups A/C (samples DTB17-05 and DTB17-11) from the overlying provenance Group B (DTB17-14) (see Figures 4 and 8), suggesting that it may be correlative to sequence boundary S3 of Link et al. (1987) shown in Figure 12. (c) Contact (dashed line) interpreted as an unconformity between the early to middle Cambrian (?) upper Clayton Mine Quartzite (provenance Group B) and the overlying Middle Ordovician Ella Dolomite (provenance Group D; see Figure 8); this suggests that upper Cambrian and Lower Ordovician rocks are missing here.

and Mutual formations). The upper ~400 m of the Clayton Mine Quartzite has similar detrital zircon populations (Group B) to the upper Brigham Group (Camelback Mountain and correlative Geertsen Canyon formations).

The Clayton Mine Quartzite is approximately one third as thick as the Brigham Group (Figure 4) in southeastern Idaho, and contains several unconformities (Figures 13a and 13b). Along Garden Creek (Figure 4), these unconformities occur between provenance Groups A and B (between DTB17-16 and DTB17-11, Figure 8). Near Clayton, Idaho, the Middle Ordovician Ella Dolomite and Kinnikinic Quartzite lie directly above the Clayton Mine Quartzite (Figure 13c; Krohe et al., 2020) suggesting that correlatives of the lower Cambrian to Lower Ordovician carbonate strata of southeastern Idaho are missing at Bayhorse (Figure 5). This represents approximately 2 km of missing strata.

Metasedimentary rocks found in the middle plate of the Pioneer core complex (Figure 2) contain detrital zircon populations (Figure 9; notably the 1.3–1.0 Ga population) similar to strata of Group A in the Bayhorse section. This is consistent with the assignment of the rocks in the core complex to the Clayton Mine Quartzite by Dover (1981). We interpret Dover's, 1983 Ygq (gneissose quartzite), Ybc (banded calc-silicate) and Yps (pelitic schist) units of the core complex to be correlative with the lower Bayhorse section, based on the identical detrital zircon populations and similar compositions. Thus, the age of these units (Dover's (1983) Ygq, Ybc, and Yps) should thus be designated Neoproterozoic rather than Mesoproterozoic.

Amphibolite-grade metasedimentary rocks exposed within the Sawtooth metamorphic complex also show similar detrital zircon populations (Ma et al., 2016) to provenance Group A of the Bayhorse section. This suggests that west of the Lemhi Arch and prior to Phanerozoic metamorphism, magmatism, and thrust faulting, Cyrogenian and Ediacaran rocks were originally widespread from Pocatello to Edwardsburg, but with significant thickness changes (Figure 2).

5.4. Comparison to Regional Detrital Zircon Trends

Combining the samples from each provenance group into one data set allowed for further evaluation of the Bayhorse strata in a regional context. We then applied the cross-correlation metric to our groupings and a regional data set of compiled Neoproterozoic to Ordovician strata (Beranek et al., 2016; Link, Todt, et al., 2017; Matthews et al., 2018; May et al., 2013; Yonkee et al., 2014; see supporting information Table S8: cross-correlation comparison for data compilation). In the cross-correlation metric, the closer the number is to 1, the more similar the samples are to one another. MDS Group A showed the greatest similarity to the Ediacaran lower Brigham Group (see Figure 10; Caddy Canyon, Inkom, and Mutual formations) with a value of 0.69. Group B showed the most similarity to the upper Brigham Group (and correlatives) with a value of 0.74. Group C did not show a strong correlation to any samples of the regional data set. Finally, Group D shows a very strong similarity to the Middle Ordovician Kinnikinic Quartzite with a value of 0.95. The Bayhorse groups show essentially no similarity to the upper Cambrian regional data set.

5.5. Interrupted Subsidence and Sedimentation

We interpret the similar parts of the newly identified Cryogenian to Ediacaran Bayhorse section and the correlative section in southeastern Idaho to record a period of Neoproterozoic extension and contemporaneous basin subsidence. This stratigraphic interval was interpreted to coincide with onset of regional subsidence during Rodinian rifting (Yonkee et al., 2014).

In southeastern Idaho, this interval of initial extension was followed by final rifting and transition to thermal subsidence around the Neoproterozoic/Cambrian boundary (Yonkee et al., 2014). This was marked by the deposition of thick Ediacaran shallow marine and fluvial siliciclastic strata overlain by Cambrian basal sandstones and thick Cambrian carbonate rocks (Matthews et al., 2018; Yonkee et al., 2014). In contrast to correlative Ediacaran quartzites of the Brigham Group, the lesser thickness of the Clayton Mine Quartzite, intermittent magmatism in central Idaho magmatism during ca. 601 and 500–490 Ma, and absence and/or dramatically reduced thickness of upper Cambrian and Lower Ordovician strata at Bayhorse suggest that the interval of final rifting in central Idaho was intermittent compared to southeastern Idaho, with significantly less subsidence. The presence of a locally sourced (665–650 Ma) detrital zircon population in the lower Clayton Mine Quartzite is interpreted to record intermittent isolation of the central Idaho margin from the margin south of the Snake River Plain, possibly coeval with the period of ca. 601 magmatism.

5.6. Development of the Neoproterozoic to Early Paleozoic Laurentian Margin

A "detachment model" of asymmetric continental rifting (Lister et al., 1986) has been applied to the western margin of Laurentia for over 20 years (Figure 14a; Cecile et al., 1997; Lund, 2008; Lund et al., 2010; Link, Todt, et al., 2017). In this context, central Idaho, north of the Snake River Plain, formed the upper plate of a major, lithospheric scale detachment fault. Though observations from modern and ancient rift margins suggest more complexity in fault and basin geometries than hypothesized by Lister et al. (1986), many observations support the first-order characteristics of the upper plate-lower plate model (e.g., Péron-Pinvidic et al., 2015).

The magma-poor Iberia-Newfoundland system demonstrates the polyphase and spatially heterogeneous nature of rifting (Beranek, 2017). This consists of different modes of extension, referred to as stretching, thinning, and exhumation, that migrate oceanward before breakup occurs, and result in the formation of distinct spatial domains, referred to as the proximal, necking, and distal domains (Figure 14b; Lavier & Manatschal, 2006; Péron-Pinvidic & Manatschal, 2009; Pereira & Alves, 2012; Péron-Pinvidic et al., 2013, 2015; Redfield & Osmundsen, 2013). Importantly, rifting is a polyphase process, rift activity migrates, and the mode of rifting and corresponding domain formation changes through time. The ability of the lithosphere to extend during continental rifting depends largely on the rates of extension and prerift rheology, such as the occurrence or absence of strong/weak layers (Huismans & Beaumont, 2002, 2008, 2011).

Applying these observations from modern margins to the Neoproterozoic margin of Idaho, we suggest that during the initial late Tonian and Cryogenian phases (~720–660 Ma) of Laurentian rifting and early regional, broad subsidence, rifting was typified by depth-independent, dominantly symmetrical rifting (Yonkee et al., 2014). This is recorded by correlative strata found ~400 km along strike of the inferred rift margin from southeastern Idaho to Edwardsburg, which is consistent with initial (dominantly pure shear) stretching. We suggest that the lower Bayhorse section and correlative strata in southeastern Idaho were deposited within the developing proximal domain during this phase (Figure 14c). The deposition of correlative strata from Bayhorse to southeastern Idaho during this interval indicates minimal variation in rift-related sedimentation, suggesting the asymmetry required to define a lower or upper plate margin was not present, and the Snake River transfer fault was not yet active.

Along the North Atlantic margin, this initial stretching phase and formation of the proximal domain was followed by drastic crustal thinning of the oceanward portion of what was initially the proximal domain during the thinning phase (analogous to what is shown in Figure 14d). This region of drastic crustal thinning is termed the necking domain. In the North Atlantic, the width of the necking domain varies from less than 50 km to greater than 150 km (Péron-Pinvidic et al., 2013). Although these differences result from multiple parameters, several studies (Manatschal et al., 2015; Mohn et al., 2012) have identified that these changes in necking domain geometry coincide with changes in the inherited rheology of the crust. Areas of more ductile crust generally show a wider necking domain, and conversely, areas of strong and more rigid crust show a

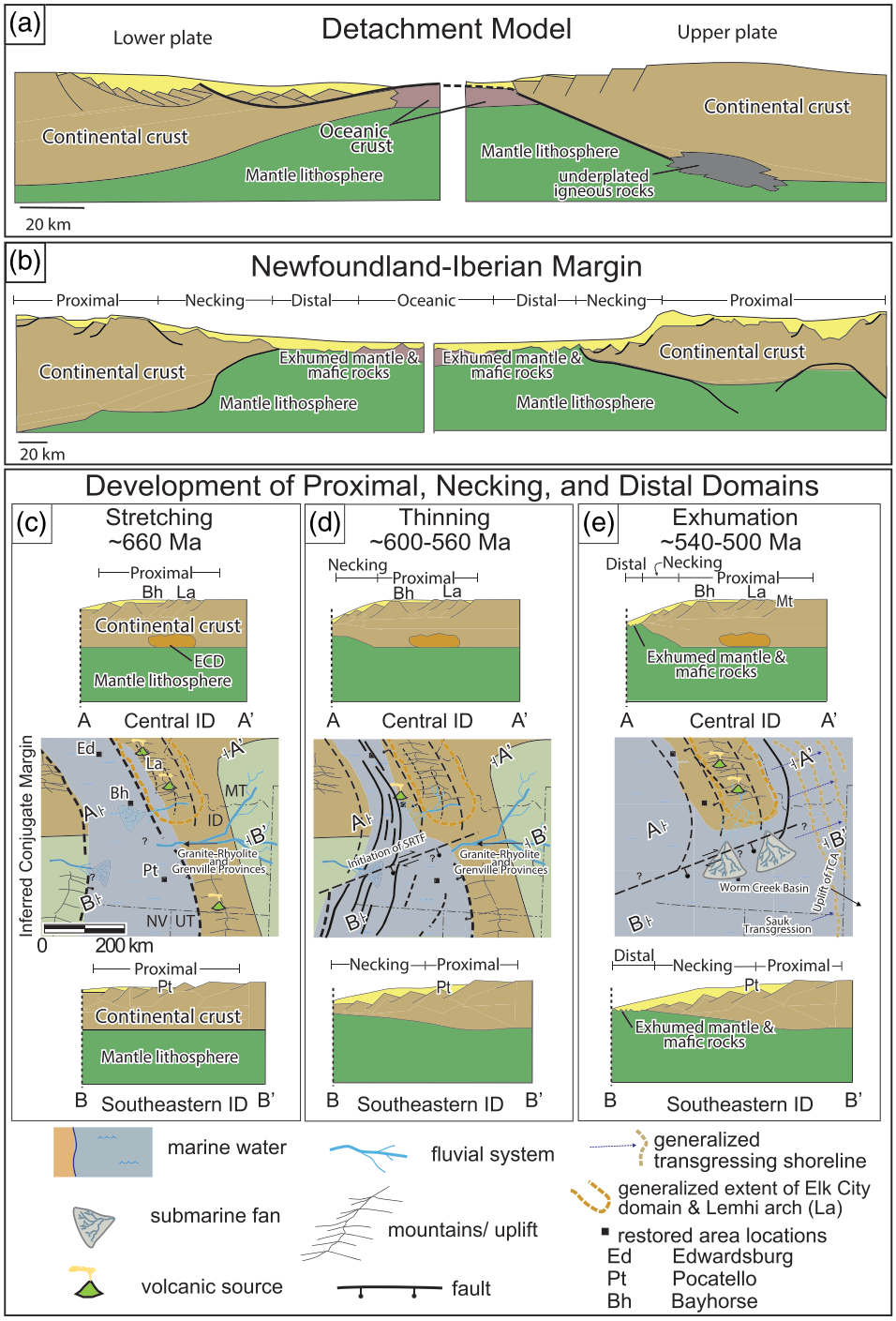

Figure 14. (a) Schematic representation of the upper and lower plate end-member margins of the detachment rifting model (after Lister et al., 1986). (b) Schematic cross sections of the Newfoundland and Iberian conjugate margins adapted from Péron-Pinvidic et al. (2013) and Campbell et al. (2019), showing heterogeneity not easily explained by the detachment model. Approximate extents of the proximal, necking, and distal domains are indicated. (c–e) Cartoons showing generalized and simplified paleogeographic map view and cross sections of the central Cordilleran margin (north and south of the modern Snake River Plain) during proposed (c) Cryogenian stretching and development of the proximal domain, (d) Ediacaran thinning, development of the necking domain, and initiation of Snake River transfer fault (SRTF), and (e) early Cambrian lithospheric breakup following a period of mantle exhumation and development of the distal domain. Note our proposed difference in geometries of the proximal and necking domains from central to southeastern Idaho (see Lavier & Manatschal, 2006; Péron-Pinvidic & Manatschal, 2009; Péron-Pinvidic et al., 2013, 2015 for further discussion of rifting processes and margin domains). Approximate extents of Elk City domain (ECD), Lemhi arch (La), Montana trough (Mt), and restored locations of Bayhorse (Bh), Pocatello (Pt), and Edwardsburg (Ed) are indicated. Paleogeographic maps and restored area locations adapted from Yonkee et al. (2014). Other abbreviations include Idaho (ID), Montana (MT), Utah (UT), Nevada (NV), and Transcontinental Arch (TCA).

narrower necking width. The amount of crustal thinning accommodated within the necking domain, from >25 down to <10 km, is relatively constant between wide and narrow necking width. Variations in necking domain width are often accommodated by transverse fault zones (e.g., Pereira et al., 2016; Péron-Pinvidic et al., 2015).

Following Beranek (2017) and Campbell et al. (2019), we suggest that the second phase of predominantly Ediacaran and early Cambrian rifting (~600–520 Ma), volcanism, and transition to drift along the Cordilleran margin (Yonkee et al., 2014) consisted of depth-dependent and asymmetric crustal thinning during formation of the necking domain (Figure 14d) and eventual lithospheric breakup (Figure 14e). During this interval, we identified significant stratigraphic differences from the newly documented sections in central Idaho and those of southeastern Idaho, including likely discontinuous sedimentation and less subsidence, as well as exhumation in east central Idaho. We propose that these differences are due to discontinuous sedimentation in central Idaho within the proximal domain, possibly reflecting formation of a relatively narrow and abrupt necking domain outboard (west) of the Bayhorse and Clayton sections, and initiation of the Snake River fault of Lund (2008).

Though 601 ± 27 Ma mafic magmatism in central Idaho (Ramshorn gabbro) is unusual relative to the most voluminous episodes of felsic magmatism along the Cordilleran margin elsewhere (Beranek, 2017; Lund et al., 2010; Madronich, 2019; Yonkee et al., 2014), other workers have reported similar Ediacaran ages for mafic rocks. In fact, Yonkee et al. (2014) described abundant but poorly dated mafic volcanic rocks and dikes in a correlative part of the section of northern Utah. The upper bound of their reported age of ~570–540 Ma was based partially upon a $^{40}Ar/^{39}Ar$ hornblende age (Crittenden & Wallace, 1973) from a trachyte flow in the Browns Hole Formation (Brigham Group), which has since been revised to ~613 Ma (Provow, 2019). A similar, but slightly younger age of 569.6 ± 5.3 Ma was obtained from U-Pb zircon dating of a trachyandesite feeder dike that sourced mafic rocks of the Hamill Group in British Columbia (Colpron et al., 2002). The ca. 601 Ma Ramshorn gabbro may thus be a manifestation of the onset of basaltic volcanism associated with late Ediacaran-early Cambrian final rifting and lithospheric breakup (e.g., Bond & Kominz, 1984; Colpron et al., 2002; Devlin, 1989; Yonkee et al., 2014). Mafic magmatism of this age may be underrepresented in the rift record along the western Laurentian margin due to analytical difficulties in dating mafic rocks.

We suggest that the thicker stratigraphic section deposited in southeastern Idaho during this Ediacaran–early Cambrian interval reflects deposition within a region that underwent more crustal subsidence than in central Idaho. This is consistent with southeastern Idaho developing a larger region of gradual crustal thinning (i.e., wider necking domain). Steeply tapering modern passive margins (i.e., narrow necking domain) have an association with higher escarpments and more exhumation within the proximal domain (Osmundsen & Redfield, 2011; Redfield & Osmundsen, 2013). This is likely because more abrupt crustal thinning concentrates isostatic unloading over a much narrower zone resulting in focused and increased isostatic uplift. In contrast, more gradual crustal thinning (i.e., wider necking domain) spreads isostatic unloading over a wider region, resulting in distributed and reduced isostatic uplift (e.g., Redfield & Osmundsen, 2013).

These differences in proposed proximal and necking domain geometries (narrow near Bayhorse, and wider to the south) may reflect differences in the prerifting crustal rheology. We suggest that large-magnitude Mesoproterozoic rifting beneath the >15 km thick Belt basin (Doughty & Chamberlain, 1996; Elk City domain of Gaschnig et al., 2013) predisposed the crust to resist Neoproterozoic to Cambrian crustal thinning (cf. Yonkee et al., 2014). The Snake River Transform zone (Link, Todt, et al., 2017; Lund, 2008) may have developed during the second phase of predominantly Ediacaran and early Cambrian rifting and separated regions with different mechanical behaviors. In modern margins, transverse fault zones often accommodate differences in necking domain geometry (Pereira et al., 2016; Péron-Pinvidic et al., 2015).

Lithospheric breakup along the central Cordilleran margin is generally thought to have occurred by middle Cambrian time (e.g., Bond et al., 1984; Yonkee et al., 2014), coinciding with a period of mantle exhumation prior to initiation of seafloor spreading (Figure 14e; Beranek, 2017). In central Idaho, our proposed narrow and abrupt necking zone associated with limited extension within the Elk City domain and focused isostatic unloading/uplift, potentially increased buoyancy due to intrusion of lower density melts of the 500–490 Ma Beaverhead plutons (Link & Janecke, 2009) and/or local sea level drop, may have all contributed to the observed general lack of subsidence in central Idaho during this interval.

6. Conclusions

An intact section of sedimentary rocks near Bayhorse in central Idaho that were formerly thought to be Ordovician in age (Hobbs et al., 1991) overlies a 667 Ma tuff and was intruded by ca. 601 Ma gabbroic sills. The strata were deposited west of the Lemhi arch, a region within the Laurentian passive margin where Neoproterozoic and Cambrian sedimentary rocks are absent. Detrital zircon age populations in the newly identified section correlate well with those in southeastern Idaho and to the northwest near Stibnite, Idaho. This suggests that Neoproterozoic stratigraphy was once continuous from southeastern Idaho through central Idaho. The primary conclusions from this study include the following:

1. The Bayhorse section lies in stratigraphic continuum above a 667 Ma tuff. Instead of previously interpreted relations that involve major thrust faults bounding structural-stratigraphic terranes, our mapping documents that quartzites (Clayton Mine Quartzite) lie above shales (Ramshorn Slate) in a gradational stratigraphic contact that was intruded by a 601 $\pm$ 27 Ma gabbro. This constrains the lower portion of the Bayhorse section to a Cryogenian to Ediacaran age.
2. The lithologies, detrital zircon populations, and volcanic ages found within the Bayhorse section are similar to those in the upper Pocatello Formation and Brigham Group of southeastern Idaho.
3. We interpret the shift from ca. 1.3–1.0 Ga to older Paleoproterozoic (ca. 1.78 Ga) detrital zircon populations within the Clayton Mine Quartzite, and complete absence of any 500–480 Ma grains, to be consistent with a middle Cambrian minimum depositional age.
4. The Middle Ordovician Ella Dolomite unconformably overlies the likely middle Cambrian Clayton Mine Quartzite, suggesting that approximately 2 km of upper Cambrian and Lower Ordovician carbonates present in the correlative southeastern Idaho sections are missing at Bayhorse.

In the context of existing work, we propose that the Neoproterozoic to lower Paleozoic stratigraphic relations between southeastern and central Idaho represents (1) an initial symmetric, predominantly Cryogenian-Ediacaran period of rifting and formation of the proximal margin domain, followed by (2) Ediacaran-early Cambrian formation of the necking domain and asymmetric, diachronous (likely accommodated by initiation of transverse faults such as the Snake River transfer fault) final rifting. The variation in Neoproterozoic tectonostratigraphic architecture was likely controlled by preexisting crustal character, in particular the 1,370 Ma region of mafic magmatism within the Elk City domain of the Belt basin. This region of mafic magmatism appears to have diverted the generally north-south trending rift margin to the northwest, around the southwestern margin of the Belt basin. The rifted-margin architecture described here implies similar rifting processes between the Neoproterozoic-Cambrian Laurentian margin and the Mesozoic North Atlantic rift.

Data Availability Statement

Data supporting the conclusions are available in the supporting information and online (at https://www.geochron.org/dataset/html/geochron_dataset_2020_05_23_Wh7fW).

Acknowledgments

Nick Krohe and Trent Armstrong analyzed the "NK" and "TA" detrital zircon samples as part of their MS (Krohe, 2016) and undergraduate theses, respectively. Much of the work described here was completed as a part of a MS thesis of Brennan (2018) at Idaho State University funded by the U.S. Geological Survey, National Cooperative Geologic Mapping Program Award GA17AC00159 to Pearson, and Geological Society of America and Idaho State University Geosciences Geslin and Thompson Endowment grants to Brennan. Brennan is currently supported by a Curtin University scholarship. The ion microprobe facility at UCLA is partly supported by a grant from the Instrumentation and Facilities Program, Division of Earth Sciences, National Science Foundation. Chamberlain was partially supported by Mega-Grant 14.Y26.31.0012 and RNF Grant 18-17-00240 of the government of the Russian Federation. We acknowledge NSF-EAR 1649254 for support of the Arizona LaserChron Center and extend a thank you to Mark Pecha, Kojo Kelty, and Chelsi White for their assistance. Elena Morozova assisted in the image preparations for SIMS dating of the Ramshorn gabbro. Mark Fanning assisted with SHRIMP analyses. J. Brian Mahoney, Molly Gallahue, and Adolph Yonkee provided helpful comments on an early draft. Thoughtful reviews by Luke Beranek and William Matthews improved the manuscript. This is a contribution to IGCP 648.

References

Amato, J. M., & Mack, G. H. (2012). Detrital zircon geochronology from the Cambrian-Ordovician Bliss sandstone, New Mexico: Evidence for contrasting Grenville-age and Cambrian sources on opposite sides of the Transcontinental Arch. *GSA Bulletin*, *124*(11–12), 1826–1840. https://doi.org/10.1130/B30657.1

Armstrong, R. L., Taubeneck, W. H., & Hales, P. O. (1977). Rb-Sr and K-Ar geochronometry of Mesozoic granitic rocks and their Sr isotopic composition, Oregon, Washington, and Idaho. *GSA Bulletin*, *88*(3), 397–411. https://doi.org/10.1130/0016-7606(1977)88<397:RAKGOM>2.0.CO;2

Audet, P., Sole, C., & Schaeffer, A. J. (2016). Control of lithospheric inheritance on Neotectonic activity in northwestern Canada? *Geology*, *44*(10), 807–810. https://doi.org/10.1130/G38118.1

Bahlburg, H., Vervoort, J. D., Andrew DuFrane, S., Carlotto, V., Reimann, C., & Cárdenas, J. (2011). The U-Pb and Hf isotope evidence of detrital zircons of the Ordovician Ollantaytambo formation, southern Peru, and the Ordovician provenance and paleogeography of southern Peru and northern Bolivia. *Journal of South American Earth Sciences*, *32*(3), 196–209. https://doi.org/10.1016/j.jsames.2011.07.002

Balgord, E. A., Yonkee, W. A., Link, P. K., & Fanning, C. M. (2013). Stratigraphic, geochronologic, and geochemical record of the Cryogenian Perry canyon formation, northern Utah: Implications for Rodinia rifting and Snowball Earth glaciation. *GSA Bulletin*, *125*(9–10), 1442–1467. https://doi.org/10.1130/B30860.1

Beranek, L. P. (2017). A magma-poor rift model for the Cordilleran margin of western North America. *Geology*, *45*(12), 1115–1118. https://doi.org/10.1130/G39265.1

Beranek, L. P., Link, P. K., & Fanning, C. M. (2016). Detrital zircon record of mid-Paleozoic convergent margin activity in the northern U.S. Rocky Mountains: Implications for the Antler orogeny and early evolution of the North American Cordillera. *Lithosphere*, *8*(5), 533–550. https://doi.org/10.1130/L557.1

Bond, G. C., & Kominz, M. A. (1984). Construction of tectonic subsidence curves for the early Paleozoic miogeocline, southern Canadian Rocky Mountains: Implications for subsidence mechanisms, age of breakup, and crustal thinning (Canada). *GSA Bulletin*, *95*(2), 155–173. https://doi.org/10.1130/0016-7606(1984)95<155:COTSCF>2.0.CO;2

Bouvier, A., Vervoort, J. D., & Patchett, P. J. (2008). The Lu-Hf and Sm-Nd isotopic composition of CHUR: Constraints from unequilibrated chondrites and implications for the bulk composition of terrestrial planets. *Earth and Planetary Science Letters*, *273*(1-2), 48–57. https://doi.org/10.1016/j.epsl.2008.06.010

Brennan, D. T. (2018). *Geologic mapping and detrital zircon provenance of the Bayhorse anticline, Custer County, Idaho: Revised Neoproterozoic to Lower Paleozoic stratigraphy (MS thesis)*. Pocatello, ID: Idaho State University. 155 p., 1 plate

Brennan, D. T., Pearson, D. M., Link, P. K., & Chamberlain, K. R. (2020). Geologic map of the Bayhorse anticline, Custer County, Idaho. In *Idaho Geological Survey Technical Report T-20-01, 1:24,000*. Moscow, ID.

Buck, W. R. (2004). Consequences of asthenospheric variability on continental rifting. In G. D. Karner, B. Taylor, N. W. Driscoll, & D. L. Kohlstedt (Eds.), *Rheology and deformation of the lithosphere at continental margins* (pp. 1–30). New York: Columbia University Press. https://doi.org/10.7312/karn12738-002

Bush, J. H., Thomas, R. C., & Pope, M. C. (2012). Sauk megasequence deposition in northeastern Washington, northern Idaho, and western Montana. In J. R. Derby, R. D. Fritz, S. A. Longacre, W. A. Morgan, & C. A. Sternbach (Eds.), *The great American carbonate bank: The geology and economic resources of the Cambrian–Ordovician Sauk megasequence of Laurentia* (Vol. 98, pp. 751–768). Tulsa, OK, USA: AAPG Memoir. https://doi.org/10.1306/13331515M983512

Campbell, R. W., Beranek, L. P., Piercey, S. J., & Friedman, R. (2019). Early Paleozoic post-breakup magmatism along the Cordilleran margin of western North America: New zircon U-Pb age and whole-rock Nd-and Hf-isotope and lithogeochemical results from the Kechika Group, Yukon, Canada. *Geosphere*, *15*(4), 1262–1290. https://doi.org/10.1130/GES02044.1

Cecile, M. P., Morrow, D. W., & Williams, G. K. (1997). Early Paleozoic (Cambrian to Early Devonian) tectonic framework, Canadian Cordillera. *Bulletin of Canadian Petroleum Geology*, *45*, 54–74. https://doi.org/10.35767/gscpgbull.45.1.054

Chamberlain, K. R., Schmitt, A. K., Swapp, S. M., Harrison, T. M., Swoboda-Colberg, N., Bleeker, W., et al. (2010). In situ U-Pb SIMS (IN-SIMS) micro-baddeleyite dating of mafic rocks: Method with examples. *Precambrian Research*, *183*(3), 379–387. https://doi.org/10.1016/j.precamres.2010.05.004

Christie-Blick, N. (1982). Upper Proterozoic and Lower Cambrian rocks of the Sheeprock Mountains, Utah: Regional correlation and significance. *GSA Bulletin*, *93*(8), 735–750. https://doi.org/10.1130/0016-7606(1982)93<735:UPALCR>2.0.CO;2

Christie-Blick, N., Grotzinger, J. P., & Von Der Borch, C. (1988). Sequence stratigraphy in Proterozoic successions. *Geology*, *16*(2), 100–104. https://doi.org/10.1130/0091-7613(1988)016<0100:SSIPS>2.3.CO;2

Collerson, K. D., Van Schmus, R. W., Lawry, J. F., & Bickford, M. E. (1988). Buried Precambrian basement in south-central Saskatchewan: Provisional results from Sm-Nd model ages and U-Pb zircon geochronology. R. Macdonald *Summary of Investigations 1988, Saskatchewan Geological Survey Miscellaneous Report* (4th ed., Vol. 88, pp. 142–150). Saskatchewan Department of Energy and Mines: Saskatchewan Geological Survey. https://doi.org/10.1017/CBO9781107415324.004

Colpron, M., Logan, J. M., & Mortensen, J. K. (2002). U-Pb zircon age constraint for late Neoproterozoic rifting and initiation of the lower Paleozoic passive margin of western Laurentia. *Canadian Journal of Earth Sciences*, *39*(2), 133–143. https://doi.org/10.1139/e01-069

Crittenden, M. D. Jr., & Wallace, C. A. (1973). Possible equivalents of the Belt Supergroup in Utah. In *Belt Symposium 1973, Volume 1* (pp. 116–138). Moscow, ID: Idaho Bureau of Mines and Geology.

Dehler, C., Gehrels, G., Porter, S., Heizler, M., Karlstrom, K., Cox, G., et al. (2017). Synthesis of the 780–740 Ma Chuar, Uinta Mountain, and Pahrump (ChUMP) groups, western USA: Implications for Laurentia-wide cratonic marine basins. *GSA Bulletin*, *129*(5–6), 607–624. https://doi.org/10.1130/B31532.1

Dehler, C. M., Fanning, C. M., Link, P. K., Kingsbury, E. M., & Rybczynski, D. (2010). Maximum depositional age and provenance of the Uinta Mountain Group and Big Cottonwood Formation, northern Utah: Paleogeography of rifting western Laurentia. *GSA Bulletin*, *122*(9–10), 1686–1699. https://doi.org/10.1130/B30094.1

Devlin, W. J. (1989). Stratigraphy and sedimentology of the Hamill Group in the northern Selkirk Mountains, British Columbia: Evidence for latest Proterozoic-Early Cambrian extensional tectonism. *Canadian Journal of Earth Sciences*, *26*(3), 515–533. https://doi.org/10.1139/e89-044

Dickinson, W. R. (2004). Evolution of the North American Cordillera. *Annual Review of Earth and Planetary Sciences*, *32*(1), 13–45. https://doi.org/10.1146/annurev.earth.32.101802.120257

Doughty, P. T., & Chamberlain, K. R. (1996). Salmon River Arch revisited: New evidence for 1370 Ma rifting near the end of deposition in the Middle Proterozoic Belt basin. *Canadian Journal of Earth Sciences*, *33*(7), 1037–1052. https://doi.org/10.1139/e96-079

Dover, J. H. (1981). Geology of the Boulder-Pioneer wilderness study area. In F. S. Simons, J. H. Dover, D. R. Mabey, E. T. Tuchek, & J. Ridenour (Eds.), *Mineral resources of the Boulder-Pioneer study area, Blaine and Custer Counties* (Vol. 1497, pp. 15–75). Idaho: U.S.: Geological Survey Bulletin.

Dover, J. H. (1983). Geologic map and sections of the central Pioneer Mountains, Blaine and Custer Counties, central Idaho. In *U.S. Geological Survey miscellaneous investigations Series Map I-1319, 1:48,000*. Denver, CO: U.S. Geological Survey.

Elison, M. W., Speed, R. C., & Kistler, R. W. (1990). Geologic and isotopic constraints on the crustal structure of the northern Great Basin. *GSA Bulletin*, *102*(8), 1077–1092. https://doi.org/10.1130/0016-7606(1990)102<1077:GAICOT>2.3.CO;2

Eriksson, K., Campbell, I., Palin, J., & Allen, C. (2003). Predominance of Grenvillian magmatism recorded in detrital zircons from modern Appalachian rivers. *The Journal of Geology*, *111*(6), 707–717. https://doi.org/10.1086/378338

Fanning, C. M., & Link, P. K. (2004). U-Pb SHRIMP ages of Neoproterozoic (Sturtian) glaciogenic Pocatello formation, southeastern Idaho. *Geology*, *32*(10), 881–884. https://doi.org/10.1130/G20609.1

Fisher, F. S., McIntyre, D. H., & Johnson, K. M. (1992). Geologic map of the Challis 1°×2° quadrangle, Idaho. In *U.S. Geological Survey miscellaneous investigations Series Map, v. I-1819, scale 1:250,000, (39)*. Denver, CO: U.S. Geological Survey.

Foster, D. A., Mueller, P. A., Mogk, D. W., Wooden, J. L., & Vogl, J. J. (2006). Proterozoic evolution of the western margin of the Wyoming craton: Implications for the tectonic and magmatic evolution of the northern Rocky Mountains. *Canadian Journal of Earth Sciences*, *43*(10), 1601–1619. https://doi.org/10.1139/e06-052

Gaschnig, R. M., Vervoort, J. D., Lewis, R. S., & Tikoff, B. (2013). Probing for Proterozoic and Archean crust in the northern U.S. Cordillera with inherited zircon from the Idaho batholith. *GSA Bulletin*, *125*(1–2), 73–88. https://doi.org/10.1130/B30583.1

Gehrels, G., & Pecha, M. (2014). Detrital zircon U-Pb geochronology and Hf isotope geochemistry of Paleozoic and Triassic passive margin strata of western North America. *Geosphere*, *10*(1), 49–65. https://doi.org/10.1130/GES00889.1

Gehrels, G. E., Valencia, V. A., & Pullen, A. (2006). Detrital zircon geochronology by laser-ablation multicollector ICPMS at the Arizona Laserchron Center. In T. Olszewski (Ed.), *Geochronology: Emerging opportunities, Paleontological Society short course, October 21, 2006* (Vol. 12, pp. 67–76). Philadelphia, PA: The Paleontological Society.

Gehrels, G. E., Valencia, V. A., & Ruiz, J. (2008). Enhanced precision, accuracy, efficiency, and spatial resolution of U-Pb ages by laser ablation-multicollector-inductively coupled plasma-mass spectrometry. *Geochemistry, Geophysics, Geosystems*, *9*. https://doi.org/10.1029/2007GC001805

Hansen, C. M. (2015). *An investigation into the Poison Creek thrust: A Sevier thrust with Proterozoic implications* (MS thesis). Pocatello, ID: Idaho State University.

Harlan, S. S., Heaman, L., LeCheminant, A. N., & Premo, W. R. (2003). Gunbarrel mafic magmatic event: A key 780 Ma time marker for Rodinia plate reconstructions. *Geology*, *31*(12), 1053–1056. https://doi.org/10.1130/G19944.1

Haupert, I., Manatschal, G., Decarlis, A., & Unternehr, P. (2016). Upper-plate magma-poor rifted margins: Stratigraphic architecture and structural evolution. *Marine and Petroleum Geology*, *69*, 241–261. https://doi.org/10.1016/j.marpetgeo.2015.10.020

Hayward, N. (2015). Geophysical investigation and reconstruction of lithospheric structure and its control on geology, structure, and mineralization in the Cordillera of northern Canada and eastern Alaska. *Tectonics*, *34*, 2165–2189. https://doi.org/10.1002/2015TC003871

Hildebrand, R. S. (2009). Did westward subduction cause Cretaceous–Tertiary orogeny in the North American Cordillera? In M. E. Bickford, & D. I. Siegel (Eds.), *Geological Society of America special paper* (Vol. 457, pp. 1–71). Boulder, CO: Geological Society of America. https://doi.org/10.1130/2009.2457

Hobbs, S. W. (1985). Precambrian and Paleozoic sedimentary terranes in the Bayhorse area of the Challis quadrangle. In D. H. McIntyre (Ed.), *Symposium on the geology and mineral deposits of the Challis 1-degree × 2-degree quadrangle, Idaho* (Vol. 1658, pp. 59–68). Alexandria, VA USA: U.S. Geological Survey Bulletin.

Hobbs, S. W., & Hays, W. H. (1990). Ordovician and older rocks of the Bayhorse area, Custer County, Idaho. In *U.S. Geological Survey Bulletin, 1891* (pp. 1–40). Denver, CO: U.S. Geological Survey.

Hobbs, S. W., Hays, W. H., & McIntyre, D. H. (1975). Geologic map of the Clayton quadrangle, Custer County, Idaho. In *U.S. Geological Survey Open-File Report 75–76, 1:62,500* (23 p.). Denver, CO: U.S. Geological Survey.

Hobbs, S. W., Hays, W. H., & McIntyre, D. H. (1991). Geologic map of the Bayhorse area, central Custer County, Idaho. In *U.S. Geological Survey miscellaneous investigations Series Map I-1882, 1:62,500* (14 p.). Denver, CO: U.S. Geological Survey.

Hobbs, S. W., Hays, W. H., & Ross, R. J. (1968). The Kinnikinic Quartzite of central Idaho—Redefinition and subdivision. In *U.S. Geological Survey Bulletin, 1254* (pp. 1–22). Washington DC: U.S. Geological Survey.

Huismans, R., & Beaumont, C. (2011). Depth-dependent extension, two-stage breakup and cratonic underplating at rifted margins. *Nature*, *473*(7345), 74–78. https://doi.org/10.1038/nature09988

Huismans, R. S., & Beaumont, C. (2002). Asymmetric lithospheric extension: The role of frictional plastic strain softening inferred from numerical experiments. *Geology*, *30*(3), 211–214. https://doi.org/10.1130/0091-7613(2002)030<0211:ALETRO>2.0.CO;2

Huismans, R. S., & Beaumont, C. (2008). Complex rifted continental margins explained by dynamical models of depth-dependent lithospheric extension. *Geology*, *36*(2), 163–166. https://doi.org/10.1130/G24231A.1

Isakson, V. H. (2017). *Geochronology of the tectonic, stratigraphic, and magmatic evolution of Neoproterozoic to early Paleozoic, North American Cordillera and Cryogenian glaciation* (PhD thesis). Boise, ID: Boise State University.

Jacob, T. (1990). Late Proterozoic(?) tuff near Challis, Idaho. In F. J. Moye (Ed.), *Geology and ore deposits of the trans-Challis fault system/Great Falls tectonic zone: Guidebook of the Fifteenth Annual Tobacco Root Geological Society Field Conference, Northwest Geology* (Vol. 19, pp. 97–106). Butte, MT: Tobacco Root Geological Society.

Jones, D. S., Barnes, C. G., Premo, W. R., & Snoke, A. W. (2011). The geochemistry and petrogenesis of the Paleoproterozoic Green Mountain arc: A composite(?), bimodal, oceanic, fringing arc. *Precambrian Research*, *185*(3–4), 231–249. https://doi.org/10.1016/j.precamres.2011.01.011

Keeley, J. A., Link, P. K., Fanning, C. M., & Schmitz, M. D. (2012). Pre- to synglacial rift-related volcanism in the Neoproterozoic (Cryogenian) Pocatello formation, SE Idaho: New SHRIMP and CA-ID-TIMS constraints. *Lithosphere*, *5*(1), 128–150. https://doi.org/10.1130/L226.1

Krohe, N. (2016). *Structural framework and detrital zircon provenance of the southern portion of the Clayton quadrangle, Custer County, Idaho*. (MS thesis). Pocatello, ID: Idaho State University. 206 p., 1 plate

Krohe, N., Brennan, D. T., Link, P. K., Pearson, D. M., & Armstrong, T. (2020). Geologic map of the southern portion of the Clayton quadrangle, Custer County, Idaho. In *Idaho Geological Survey Technical Report T-20-02, 1:24,000*. Moscow ID: Idaho Geological Survey.

Lavier, L. L., & Manatschal, G. (2006). A mechanism to thin the continental lithosphere at magma-poor margins. *Nature*, *440*(7082), 324–328. https://doi.org/10.1038/nature04608

Levy, M., & Christie-Blick, N. (1991). Tectonic subsidence of the early Paleozoic passive continental margin in eastern California and southern Nevada. *GSA Bulletin*, *103*(12), 1590–1606. https://doi.org/10.1130/0016-7606(1991)103<1590:TSOTEP>2.3.CO;2

Levy, M., Christie-Blick, N., & Link, P. K. (1994). In R. W. Dalrymple, R. Boyd, & B. A. Zaitlin (Eds.), Neoproterozoic incised valleys of the eastern Great Basin, Utah and Idaho: Fluvial response to changes in depositional base level, *Incised valley systems: Origin and sedimentary sequences* (Vol. 51, pp. 369–382). McLean, VA USA: SEPM (Society for Sedimentary Geology) Special Publication.

Lewis, R. S., Link, P. K., Stanford, L. R., & Long, S. P. (2012). Geologic map of Idaho. In *Idaho Geological Survey Map M-9, scale 1:750,000* (18). Moscow, ID: Idaho Geological Survey.

Lewis, R. S., Vervoort, J. D., Burmester, R. F., & Oswald, P. J. (2010). Detrital zircon analysis of Mesoproterozoic and Neoproterozoic metasedimentary rocks of north-central Idaho: Implications for development of the Belt–Purcell basin. *Canadian Journal of Earth Sciences*, *47*(11), 1383–1404. https://doi.org/10.1139/E10-049

Linde, G. M., Cashman, P. H., Trexler, J. H., & Dickinson, W. R. (2014). Stratigraphic trends in detrital zircon geochronology of upper Neoproterozoic and Cambrian strata, Osgood Mountains, Nevada, and elsewhere in the Cordilleran miogeocline: Evidence for early Cambrian uplift of the Transcontinental Arch. *Geosphere*, *10*(6), 1402–1410. https://doi.org/10.1130/GES01048.1

Linde, G. M., Trexler, J. H., Cashman, P. H., Gehrels, G., & Dickinson, W. R. (2017). Three-dimensional evolution of the early Paleozoic western Laurentian margin: New insights from detrital zircon U-Pb geochronology and Hf isotope geochemistry of the Harmony Formation of Nevada. *Tectonics*, *36*, 2347–2369. https://doi.org/10.1002/2017TC004520

Link, P. K. (1987). The Late Proterozoic Pocatello Formation: A record of continental rifting and glacial marine sedimentation, Portneuf Narrows, southeastern Idaho. In S. S. Beus (Ed.), *Centennial field guide Volume 2: Rocky Mountain section of the Geological Society of America, decade of North American geology* (pp. 139–142). Boulder, CO: Geological Society of America.

Link, P. K., Autenrieth-Durk, K. M., Cameron, A., Fanning, C. M., Vogl, J. J., & Foster, D. A. (2017). U-Pb zircon ages of the Wildhorse gneiss, Pioneer Mountains, south-central Idaho, and tectonic implications. *Geosphere*, *13*(3), 681–698. https://doi.org/10.1130/GES01418.1

Link, P. K., Christie-Blick, N., Devlin, W. J., Elston, D. P., Horodyski, R. J., Levy, M., et al. (1993). Middle and Late Proterozoic stratified rocks of the western U.S. Cordillera, Colorado Plateau, and Basin and Range Province. In J. C. Reed, Jr., M. E. Bickford, R. S. Houston, P. K. Link, D. W. Rankin, P. K. Sims, & W. R. van Schmus (Eds.), *Precambrian: Conterminous U.S* (Vol. C-2, pp. 463–595). Boulder, Colorado: Geological Society of America, Geology of North America. https://doi.org/10.1130/DNAG-GNA-C2.463

Link, P. K., Fanning, C. M., & Beranek, L. P. (2005). Reliability and longitudinal change of detrital-zircon age spectra in the Snake River system, Idaho and Wyoming: An example of reproducing the bumpy barcode. *Sedimentary Geology*, *182*(1–4), 101–142. https://doi.org/10.1016/j.sedgeo.2005.07.012

Link, P. K., & Janecke, S. U. (2009). Mantle drip from the rising Lemhi Arch: 500 Ma plutons and detrital zircons in upper Cambrian sandstones, eastern Idaho. *Geological Society of America Abstracts with Programs*, *41*(7), 181.

Link, P. K., Jansen, S. T., Halimdihardja, P., Lande, A., & Zahn, P. (1987). Stratigraphy of the Brigham Group (Late Proterozoic–Cambrian), Bannock, Portneuf, and Bear River Ranges, southeastern Idaho. In W. R. Miller (Ed.), *The Thrust belt revisited: Thirty-eighth Field Conference, Wyoming Geological Association guidebook* (pp. 133–148). Laramie, WY: Wyoming Geological Association.

Link, P. K., Steel, T. D., Stewart, E. S., Sherwin, J., Hess, L. R., & McDonald, C. (2016). Detrital zircons in the Mesoproterozoic upper Belt Supergroup in the Pioneer, Beaverhead, and Lemhi Ranges, Montana and Idaho: The Big White arc. In J. S. Maclean, & J. W. Sears (Eds.), *Belt basin: Window to Mesoproterozoic Earth: Geological Society of America special paper* (Vol. 522, pp. 163–183). Boulder, CO. https://doi.org/10.1130/2016.2522(07)

Link, P. K., Todt, M. K., Pearson, D. M., & Thomas, R. C. (2017). 500–490 Ma detrital zircons in Upper Cambrian Worm Creek and correlative sandstones, Idaho, Montana, and Wyoming: Magmatism and tectonism within the passive margin. *Lithosphere*, *9*(6), 910–926. https://doi.org/10.1130/L671.1

Lister, G. S., Etheridge, M. A., & Symonds, P. A. (1986). Detachment faulting and the evolution of passive continental margins. *Geology*, *14*(3), 246–250. https://doi.org/10.1130/0091-7613(1986)14<246:DFATEO>2.0.CO

Ludwig, K. R. (2003). *Isoplot/Ex 3.00: A geochronological toolkit for Microsoft Excel* (Vol. 4, p. 73). Berkeley: *Berkeley Geochronology Center Special Publication*.

Lund, K. (2008). Geometry of the Neoproterozoic and Paleozoic rift margin of western Laurentia: Implications for mineral deposit settings. *Geosphere*, *4*(2), 429–444. https://doi.org/10.1130/GES00121.1

Lund, K., Aleinikoff, J. N., Evans, K. V., duBray, E. A., Dewitt, E. H., & Unruh, D. M. (2010). SHRIMP U-Pb dating of recurrent Cryogenian and Late Cambrian-Early Ordovician alkalic magmatism in central Idaho: Implications for Rodinian rift tectonics. *GSA Bulletin*, *122*(3–4), 430–453. https://doi.org/10.1130/B26565.1

Lund, K., Aleinikoff, J. N., Evans, K. V., & Fanning, C. M. (2003). SHRIMP U-Pb geochronology of Neoproterozoic Windermere Supergroup, central Idaho: Implications for rifting of western Laurentia and synchroneity of Sturtian glacial deposits. *GSA Bulletin*, *115*(3), 349–372. https://doi.org/10.1130/0016-7606(2003)115<0349:SUPGON>2.0.CO;2

Ma, C., Bergeron, P., Foster, D. A., Dutrow, B. L., Mueller, P. A., & Allen, C. (2016). Detrital-zircon geochronology of the Sawtooth metamorphic complex, Idaho: Evidence for metamorphosed lower Paleozoic shelf strata within the Idaho batholith. *Geosphere*, *12*(4), 1136–1153. https://doi.org/10.1130/GES01201.1

Madronich, L. I. (2019). *Detrital zircon U-Pb ages and trace element compositions from Cambrian rocks of western North America* (MS thesis). Alberta, Canada: University of Calgary. s125 p

Mahon, R. C., Dehler, C. M., Link, P. K., Karlstrom, K. E., & Gehrels, G. E. (2014). Geochronologic and stratigraphic constraints on the Mesoproterozoic and Neoproterozoic Pahrump Group, Death Valley, California: A record of the assembly, stability, and breakup of Rodinia. *GSA Bulletin*, *126*(5–6), 652–664. https://doi.org/10.1130/B30956.1

Malone, D., Craddock, J., & Kenderes, S. (2017). Detrital zircon geochronology and provenance of the Middle Cambrian Flathead sandstone, Park County, Wyoming. *The Mountain Geologist*, *52*(2), 86–103. https://doi.org/10.31582/rmag.mg.54.2.86

Manatschal, G., Lavier, L., & Chenin, P. (2015). The role of inheritance in structuring hyperextended rift systems: Some considerations based on observations and numerical modeling. *Gondwana Research*, *27*(1), 140–164. https://doi.org/10.1016/j.gr.2014.08.006

Matthews, W., Guest, B., & Madronich, L. (2018). Latest Neoproterozoic to Cambrian detrital zircon facies of western Laurentia. *Geosphere*, *14*(1), 243–264. https://doi.org/10.1130/GES01544.1

May, S. R., Gray, G. G., Summa, L. L., Stewart, N. R., Gehrels, G. E., & Pecha, M. (2013). Detrital zircon geochronology from the Bighorn Basin, Wyoming, USA: Implications for tectonostratigraphic evolution and paleogeography. *GSA Bulletin*, *125*(9-10), 1403–1422. https://doi.org/10.1130/B30824.1

McIntyre, D. H., Ekren, E. D., & Hardyman, R. F. (1982). *Stratigraphic and structural framework of the Challis volcanics in the eastern half of the Challis 1 × 2 quadrangle, Idaho* (Vol. 26, pp. 155–177). Moscow, ID: Bulletin of Idaho Bureau of Mines and Geology.

McIntyre, D. H., & Hobbs, S. W. (1987). Geologic map of the Challis Quadrangle, Custer and Lemhi Counties, Idaho. In *U.S. Geological Survey Geologic Quadrangle Map GQ-1599, 1:62,500* (75 p.). Boulder CO: U.S. Geological Survey.

McKenzie, D. (1978). Some remarks on the development of sedimentary basins. *Earth and Planetary Science Letters*, *40*, 25–32. https://doi.org/10.1016/0012-821X(78)90071-7

McMechan, M. E. (2012). Deep transverse basement structural control of mineral systems in the southeastern Canadian Cordillera. *Canadian Journal of Earth Sciences*, *49*(5), 693–708. https://doi.org/10.1139/e2012-013

Millonig, L. J., Gerdes, A., & Groat, L. A. (2012). U-Th-Pb geochronology of meta-carbonatites and meta-alkaline rocks in the southern Canadian Cordillera: A geodynamic perspective. *Lithos*, *152*, 202–217. https://doi.org/10.1016/j.lithos.2012.06.016

Mohn, G., Manatschal, G., Beltrando, M., Masini, E., & Kusznir, N. (2012). Necking of continental crust in magma-poor rifted margins: Evidence from the fossil Alpine Tethys margins. *Tectonics*, *31*. https://doi.org/10.1029/2011TC002961

Montoya, L. M. (2019). *Investigation of structural style within the Sevier fold-thrust belt along the southwestern boundary of the Lemhi arch, central Idaho* (MS thesis). Pocatello, ID: Idaho State University.

Moynihan, D. P., Strauss, J. V., Nelson, L. L., & Padget, C. D. (2019). Upper Windermere Supergroup and the transition from rifting to continent-margin sedimentation, Nadaleen River area, northern Canadian Cordillera. *GSA Bulletin*, *131*(9-10), 1673–1701. https://doi.org/10.1130/b32039.1

Mueller, P. A., Foster, D. A., Mogk, D. W., Wooden, J. L., Kamenov, G. D., & Vogl, J. J. (2007). Detrital mineral chronology of the Uinta Mountain Group: Implications for the Grenville flood in southwestern Laurentia. *Geology*, *35*(5), 431–434. https://doi.org/10.1130/G23148A.1

Mueller, P. A., Heatherington, A. L., Kelly, D. M., Wooden, J. L., & Mogk, D. W. (2002). Paleoproterozoic crust within the Great Falls tectonic zone: Implications for the assembly of southern Laurentia. *Geology*, *30*(2), 127–130. https://doi.org/10.1130/0091-7613(2002)030<0127:PCWTGF>2.0.CO;2

Mueller, P. A., Wooden, J. L., Mogk, D. W., & Foster, D. A. (2011). Paleoproterozoic evolution of the Farmington zone: Implications for terrane accretion in southwestern Laurentia. *Lithosphere*, *3*(6), 401–408. https://doi.org/10.1130/L161.1

Nordsvan, A. R., Kirscher, U., Kirkland, C. L., Barham, M., & Brennan, D. T. (2020). Resampling (detrital) zircon age distributions for accurate multidimensional scaling solutions. *Earth-Science Reviews*, *204*, 103149. https://doi.org/10.1016/j.earscirev.2020.103149

Osmundsen, P. T., & Redfield, T. F. (2011). Crustal taper and topography at passive continental margins. *Terra Nova*, *23*(6), 349–361. https://doi.org/10.1111/j.1365-3121.2011.01014.x

Patton, W. W. (1948). *Geology of the Clayton area, Custer County, Idaho* (MS thesis). Ithaca, NY: Cornell University. 43 p

Pearson, D. M., & Link, P. K. (2017). Field guide to the Lemhi arch and Mesozoic-early Cenozoic faults and folds in east-central Idaho: Beaverhead Mountains. *Northwestern Geology*, *46*, 101–112.

Pearson, D. M., Link, P. K., Todt, M. K., Hansen, C. M., Krohe, N. J., & Mahoney, J. B. (2016). The Lemhi arch of east-central Idaho: A stranded fault block within the western Laurentian rift margin. *Geological Society of America Abstracts with Programs*, *48*(5). https://doi.org/10.1130/abs/2016RM-276022

Pereira, R., & Alves, T. M. (2012). Tectono-stratigraphic signature of multiphased rifting on divergent margins (deep-offshore southwest Iberia, North Atlantic). *Tectonics*, *31*. https://doi.org/10.1029/2011TC003001

Pereira, R., Alves, T. M., & Mata, J. (2016). Alternating crustal architecture in west Iberia: A review of its significance in the context of NE Atlantic rifting. *Journal of the Geological Society*, *174*(3), 522–540. https://doi.org/10.1144/jgs2016-050

Péron-Pinvidic, G., & Manatschal, G. (2009). The final rifting evolution at deep magma-poor passive margins from Iberia-Newfoundland: A new point of view. *International Journal of Earth Sciences*, *98*(7), 1581–1597. https://doi.org/10.1007/s00531-008-0337-9

Péron-Pinvidic, G., Manatschal, G., Masini, E., Sutra, E., Flament, J. M., Haupert, I., & Unternehr, P. (2015). Unravelling the along-strike variability of the Angola–Gabon rifted margin: A mapping approach. In T. S. Ceraldi, R. A. Hodgkinson, & G. Backe (Eds.), *Petroleum geoscience of the West African margin* (Vol. 438, pp. 49–76). London, UK: Geological Society, London, Special Publications. https://doi.org/10.1144/SP438.1

Péron-Pinvidic, G., Manatschal, G., & Osmundsen, P. T. (2013). Structural comparison of archetypal Atlantic rifted margins: A review of observations and concepts. *Marine and Petroleum Geology*, *43*, 21–47. https://doi.org/10.1016/j.marpetgeo.2013.02.002

Price, R. A. (1964). The Precambrian Purcell system in the Rocky Mountains of southern Alberta and British Columbia. *Bulletin of Canadian Petroleum Geology*, *12*, 399–426.

Provow, A. (2019). *Ediacaran depositional age and subsequent fluid-rock interactions in the Mutual and Browns Hole Formations of northern Utah*. (MS thesis). Logan, UT: Utah State University. 85 p

Pullen, A., Ibáñez-Mejia, M., Gehrels, G. E., Giesler, D., & Pecha, M. (2018). Optimization of a laser ablation-single collector-inductively coupled plasma-mass spectrometer (Thermo Element 2) for accurate, precise, and efficient zircon U-Th-Pb geochronology. *Geochemistry, Geophysics, Geosystems*, *19*(10), 3689–3705. https://doi.org/10.1029/2018GC007889

Pyle, L. J., & Barnes, C. R. (2003). Lower Paleozoic stratigraphic and biostratigraphic correlations in the Canadian Cordillera: Implications for the tectonic evolution of the Laurentian margin. *Canadian Journal of Earth Sciences*, *40*(12), 1739–1753. https://doi.org/10.1139/e03-049a

Rainbird, R., Cawood, P., & Gehrels, G. E. (2012). The great Grenvillian sedimentation episode: Record of supercontinent Rodinia's assembly. In C. Busby, & A. Antonio (Eds.), *Tectonics of sedimentary basins: Recent advances* (pp. 583–601). Chichester, UK: John Wiley and Sons, ltd. https://doi.org/10.1002/9781444347166.ch29

Rainbird, R. H., Rayner, N. M., Hadlari, T., Heaman, L. M., Ielpi, A., Turner, E. C., & MacNaughton, R. B. (2017). Zircon provenance data record the lateral extent of pancontinental, early Neoproterozoic rivers and erosional unroofing history of the Grenville orogen. *GSA Bulletin*, *129*, 1408–1423. https://doi.org/10.1130/B31695.1

Redfield, T. F., & Osmundsen, P. T. (2013). The long-term topographic response of a continent adjacent to a hyperextended margin: A case study from Scandinavia. *GSA Bulletin*, *125*(1–2), 184–200. https://doi.org/10.1130/B30691.1

Reed, J. C., Bickford, M. E., Premo, W. R., Aleinikoff, J. N., & Pallister, J. S. (1987). Evolution of the Early Proterozoic Colorado province: Constraints from U-Pb geochronology. *Geology*, *15*(9), 861–865. https://doi.org/10.1130/0091-7613(1987)15<861:EOTEPC>2.0.CO;2

Roots, C. F., & Thompson, R. I. (1992). Long-lived basement weak zones and their role in extensional magmatism in the Ogilvie Mountains, Yukon Territory. In M. J. Bartholomew, D. W. Hyndman, D. W. Mogk, & R. Mason (Eds.), *Basement tectonics and characterization of ancient and Mesozoic continental margins: Proceedings of the 8th International Conference in Basement Tectonics* (pp. 359–372). Dordrecht: Kluwer Academic Publishers.

Ross, C. P. (1937). *Geology and ore deposits of the Bayhorse region, Custer County, Idaho* (Vol. 877, 161 p.), Washington DC, USA: U.S. Geological Survey Bulletin.

Ross, G. M. (1991). Tectonic setting of the Windermere Supergroup revisited. *Geology*, *19*(11), 1125–1128. https://doi.org/10.1130/0091-7613(1991)019<1125:TSOTWS>2.3.CO;2

Ross, G. M., & Parrish, R. R. (1991). Detrital zircon geochronology of metasedimentary rocks in the southern Omineca Belt, Canadian Cordillera. *Canadian Journal of Earth Sciences*, *28*(8), 1254–1270. https://doi.org/10.1139/e91-112

Ross, G. M., Parrish, R. R., Villeneuve, M. E., & Bowring, S. A. (1991). Geophysics and geochronology of the crystalline basement of the Alberta Basin, western Canada. *Canadian Journal of Earth Sciences*, *28*(4), 512–522. https://doi.org/10.1139/e91-045

Ruppel, E. T. (1986). The Lemhi Arch: A Late Proterozoic and Early Paleozoic landmass in central Idaho. In J. A. Peterson (Ed.), *Paleotectonics and sedimentation in the Rocky Mountain region, United States* (Vol. 41, pp. 119–130). Tulsa, OK: American Association of Petroleum Geologists Memoir. https://doi.org/10.1306/M41456C6

Saylor, J. E., & Sundell, K. E. (2016). Quantifying comparison of large detrital geochronology data sets. *Geosphere*, *12*(1), 203–220. https://doi.org/10.1130/GES01237.1

Schmidt, K. L., Lewis, R. S., Vervoort, J. D., Stetson-Lee, T. A., Michels, Z. D., & Tikoff, B. (2017). Tectonic evolution of the Syringa embayment in the central North American Cordilleran accretionary boundary. *Lithosphere*, *9*(2), 184–204. https://doi.org/10.1130/L545.1

Schmitt, A. K., Chamberlain, K. R., Swapp, S. M., & Harrison, T. M. (2010). In situ U–Pb dating of micro-baddeleyite by secondary ion mass spectrometry. *Chemical Geology*, *269*(3–4), 386–395. https://doi.org/10.1016/j.chemgeo.2009.10.013

Scholten, R. (1957). Paleozoic evolution of the geosynclinal margin north of the Snake River Plain, Idaho-Montana. *GSA Bulletin*, *68*(2), 151–170. https://doi.org/10.1130/0016-7606(1957)68[151:PEOTGM]2.0.CO;2

Schwartz, J. J., Johnson, K., Mueller, P., Valley, J., Strickland, A., & Wooden, J. L. (2014). Time scales and processes of Cordilleran batholith construction and high-Sr/Y magmatic pulses: Evidence from the Bald Mountain batholith, northeastern Oregon. *Geosphere*, *10*(6), 1456–1481. https://doi.org/10.1130/0016-7606(1957)68[151:PEOTGM]2.0.CO;2

Sears, J. W. (2007). Belt-Purcell Basin: Keystone of the Rocky Mountain fold-and-thrust belt, United States and Canada. In J. W. Sears, T. A. Harms, & C. A. Evenchick (Eds.), *Whence the Mountains? Inquiries into the evolution of orogenic systems: A volume in honor of Raymond A. Price: Geological Society of America Special Paper* (Vol. 433, pp. 147–166). Boulder, CO: Geological Society of America. https://doi.org/10.1130/2007.2433(07)

Sloss, L. L. (1950). Paleozoic sedimentation in Montana area. *Bulletin of the American Association of Petroleum Geologists*, *34*(3), 423–451. https://doi.org/10.1306/3D933EF0-16B1-11D7-8645000102C1865D

Sloss, L. L. (1954). Lemhi Arch, a mid-Paleozoic positive element in south-central Idaho. *GSA Bulletin*, *65*, 365–368. https://doi.org/10.1130/0016-7606(1954)65[365:LAAMPE]2.0.CO;2

Sloss, L. L. (1963). Sequences in the cratonic interior of North America. *GSA Bulletin*, *74*(2), 93–114. https://doi.org/10.1130/0016-7606(1963)74[93:SITCIO]2.0.CO;2

Söderlund, U., & Johansson, L. (2002). A simple way to extract baddeleyite (ZrO2). *Geochemistry, Geophysics, Geosystems*, *3*(2). https://doi.org/10.1029/2001GC000212

Spencer, C. J., & Kirkland, C. L. (2016). Visualizing the sedimentary response through the orogenic cycle: A multidimensional scaling approach. *Lithosphere*, *8*(1), 29–37. https://doi.org/10.1130/L479.1

Spencer, C. J., Kirkland, C. L., Roberts, N. M. W., Evans, N. J., & Liebmann, J. (2019). Strategies towards robust interpretations of in situ zircon Lu–Hf isotope analyses. *Geoscience Frontiers*, *11*(3), 843–853. https://doi.org/10.1016/j.gsf.2019.09.004

Spencer, C. J., Prave, A. R., Cawood, P. A., & Roberts, N. M. W. (2014). Detrital zircon geochronology of the Grenville/Llano foreland and basal Sauk Sequence in west Texas, USA. *GSA Bulletin*, *126*(7–8), 1117–1128. https://doi.org/10.1130/B30884.1

Stewart, D. E., Stewart, E. D., Lewis, R. S., Weppner, K. N., Isakson, V. H., & Freed, J. S. (2016). Geologic map of the Stibnite quadrangle, Valley County, Idaho. In *Idaho Geological Survey, 1:24,000*. Moscow ID: Idaho Geological Survey.

Stewart, J. H. (1972). Initial deposits in the Cordilleran geosyncline: Evidence of a Late Precambrian (<850 m.y.) continental separation. *GSA Bulletin*, *83*(5), 1345–1360. https://doi.org/10.1130/0016-7606(1972)83[1345:IDITCG]2.0.CO;2

Trimble, D. E. (1976). Geology of the Michaud and Pocatello Quadrangles, Bannock and Power Counties, Idaho. In *U.S. Geological Survey Bulletin, 1400* (88 p.). Washington, DC: U.S. Geological Survey. https://doi.org/10.3133/b1400

Turner, R. J. W., Madrid, R. J., & Miller, E. L. (1989). Roberts Mountains allochthon: Stratigraphic comparison with Lower Paleozoic outer continental margin strata of the northern Canadian Cordillera. *Geology*, *17*(4), 341–344. https://doi.org/10.1130/0091-7613(1989)017<0341:RMASCW>2.3.CO;2

Vermeesch, P. (2013). Multi-sample comparison of detrital age distributions. *Chemical Geology*, *341*, 140–146. https://doi.org/10.1016/j.chemgeo.2013.01.010

Vervoort, J. D., Lewis, R. S., Fisher, C., Gaschnig, R. M., Jansen, A. C., & Brewer, R. (2016). Neoarchean and Paleoproterozoic crystalline basement rocks of north-central Idaho: Constraints on the formation of western Laurentia. *GSA Bulletin*, *128*(1–2), B31150.1–B31150.109. https://doi.org/10.1130/B31150.1

Vervoort, J. D., Patchett, P. J., Blichert-toft, J., & Albare, F. (1999). Relationships between Lu–Hf and Sm–Nd isotopic systems in the global sedimentary system. *Earth and Planetary Science Letters*, *168*(1-2), 79–99. https://doi.org/10.1016/S0012-821X(99)00047-3

Wernicke, B. (1985). Uniform-sense normal simple shear of the continental lithosphere. *Canadian Journal of Earth Sciences*, *22*(1), 108–125. https://doi.org/10.1139/e85-009

Whitmeyer, S. J., & Karlstrom, K. E. (2007). Tectonic model for the Proterozoic growth of North America. *Geosphere*, *3*(4), 220–259. https://doi.org/10.1130/GES00055.1

Williams, I. S. (1998). U-Th-Pb geochronology by ion microprobe. In M. A. McKibben, W.C. Shanks III, & W.I. Ridley, et al. (Eds.), *Applications of microanalytical techniques to understanding mineralizing processes: Reviews in economic geology* (Vol. 7, pp. 1–35). Littleton, CO: Society of Economic Geologists. https://doi.org/10.5382/Rev.07.01

Wingate, M. T. D., & Compston, W. (2000). Crystal orientation effects during ion microprobe U-Pb analysis of baddeleyite. *Chemical Geology*, *168*(1–2), 75–97. https://doi.org/10.1016/S0009-2541(00)00184-4

Winston, D. (1986). Sedimentology of the Ravalli Group, Middle Belt Carbonate and Missoula Group, Middle Proterozoic Belt Supergroup, Montana, Idaho and Washington. In S. M. Roberts (Ed.), *Belt Supergroup: A guide to Proterozoic rocks of western Montana and adjacent areas* (Vol. 94, pp. 69–84). Butte, MT: Montana Bureau of Mines and Geology Special Publication.

Yonkee, W. A., Dehler, C. D., Link, P. K., Balgord, E. A., Keeley, J. A., Hayes, D. S., et al. (2014). Tectono-stratigraphic framework of Neoproterozoic to Cambrian strata, west-central U.S.: Protracted rifting, glaciation, and evolution of the North American Cordilleran margin. *Earth-Science Reviews*, *136*, 59–95. https://doi.org/10.1016/j.earscirev.2014.05.004

Young, G. M., Jefferson, C. W., Delaney, G. D., & Yeo, G. M. (1979). Middle and Late Proterozoic evolution of the northern Canadian Cordillera and Shield. *Geology*, *7*(3), 125–128. https://doi.org/10.1130/0091-7613(1979)7